



Multiple oxygen (^{16}O , ^{17}O and ^{18}O) and sulfur (^{32}S , ^{33}S , ^{34}S and ^{36}S) isotope signatures of the dissolved sulfate from Deception Island, Antarctic Peninsula: Implications on sulfate formation, transportation and deposition in the Antarctic region

Yeongmin Kim^a, Insung Lee^a, Jung Hun Seo^{b,*}, Jong Ik Lee^c, James Farquhar^d

^a School of Earth and Environmental Sciences, Seoul National University, Seoul 08826, Republic of Korea

^b Department of Energy and Resources Engineering, Inha University, Incheon, Republic of Korea

^c Division of Polar Earth-system Sciences, Korea Polar Research Institute, Incheon 21990, Republic of Korea

^d Department of Geology, University of Maryland, College Park, MD 20742, USA

ARTICLE INFO

Keywords:

Dissolved sulfate
Surface freshwater
Multiple oxygen isotopes
Multiple sulfur isotopes
Sulfate sources
Deception Island

ABSTRACT

Oxygen (^{16}O , ^{17}O and ^{18}O) and sulfur (^{32}S , ^{33}S , ^{34}S and ^{36}S) isotope ratios of and major ion (Na^+ , Ca^{2+} , Cl^- , NO_3^- and SO_4^{2-}) concentrations in lakes, ponds and creeks from Deception Island, Antarctic Peninsula were analyzed to study the sources of sulfate, its oxidation, and the surficial processes of the dissolved sulfate. The positive relationship between the $\delta^{34}\text{S}_{\text{sulfate}}$ (8.1‰ to 17.3‰) and the $\text{Cl}^-/\text{SO}_4^{2-}$ molar ratio suggests mixing of sulfate from atmospheric deposition and from oxidation of sulfide minerals. The average sea salt fraction (28%) and $\delta^{34}\text{S}_{\text{SS}}$ values (from 5.6‰ to 15.9‰) indicate that a combination of sea salt and marine biogenic sulfide provide the high $\delta^{34}\text{S}$ end-member of the dissolved sulfates. The relatively low $\delta^{18}\text{O}_{\text{sulfate}}$ (from -4.6 ‰ to 0.7 ‰) of Deception Island water suggests a role of local water in the formation of sulfate. Slightly negative but mass-dependent $\Delta^{17}\text{O}_{\text{sulfate}}$ values imply that atmospheric oxidation by O_3 and H_2O_2 are negligible, while these values might suggest a significant role of oxidation by molecular oxygen and $\cdot\text{OH}$. The distinctly low $\delta^{34}\text{C}_{\text{sulfate}}$ value of two samples (DCW-2 and DCW-3) suggests the input of sulfate from sulfide oxidation. Slight elevation of $\delta^{34}\text{S}_{\text{sulfate}}$ values up to 17.3‰ compared to a typical atmospheric value indicates a minimal role for dissimilatory microbial sulfate reduction of Deception Island water and sediments. Both $\Delta^{33}\text{S}_{\text{sulfate}}$ and $\Delta^{36}\text{S}_{\text{sulfate}}$ values are homogeneous and near zero, implying that the dominant atmospheric oxidation process is tropospheric and that there are minimal to no contributions of stratospheric sulfate to Deception Island water.

1. Introduction

The sulfate ion (SO_4^{2-}) is a major species in seawater and a significant component of atmospheric aerosols (Krouse and Mayer, 2000; Berner and Berner, 2012; Bao, 2015). Atmospheric sulfate aerosols are generated by various natural processes such as sea salt spray, volcanic eruption, oxidation of reduced sulfur compounds such as DMS (dimethyl sulfide) (Krouse and Mayer, 2000), dissolution of evaporite minerals (Otero et al., 2008; Rock and Mayer, 2009; Tuttle et al., 2009), sulfide oxidation (Rock and Mayer, 2009; Yuan and Mayer, 2012), as well as from anthropogenic sulfate discharge (Otero et al., 2008; Hosono et al., 2011a) and by the oxidation of atmospheric SO_2 . The oxidation of atmospheric SO_2 occurs in both the gas phase (Stockwell and Calvert, 1983) and aqueous phase (Schwartz, 1987).

Dissolved sulfate in surficial freshwater derives from deposition of

atmospheric aerosols. Both dry and wet deposition contribute this sulfate and thus atmospheric deposition can constitute an important sulfur source to groundwater (Hosono et al., 2011b; Brenot et al., 2015), rivers (Killingsworth and Bao, 2015; Li et al., 2015), and glaciers (Patris et al., 2000; Alexander et al., 2003; Kunasek et al., 2010).

The isotopic ratios of the sulfate can be represented as five different delta values, such as $\delta^{18}\text{O}$, $\Delta^{17}\text{O}$, $\delta^{34}\text{S}$, $\Delta^{33}\text{S}$ and $\Delta^{36}\text{S}$ (see the Sample and Method section for definitions of notation). Sulfate exchanges its oxygen atoms only at high temperature (350°C) and/or acidic (1 m H_2SO_4 or HCl solution) conditions (Kusakabe and Robinson, 1977; Chiba et al., 1981). Thus once formed, dissolved sulfate does not exchange oxygen with water under ambient surface conditions (Krouse and Mayer, 2000). However, biological cycling of sulfate by processes such as dissimilatory microbial sulfate reduction can allow for isotopic exchange (Llyod, 1967; Fritz et al., 1989; Van Stempvoort and Krouse,

* Corresponding author.

E-mail address: seo@inha.ac.kr (J.H. Seo).

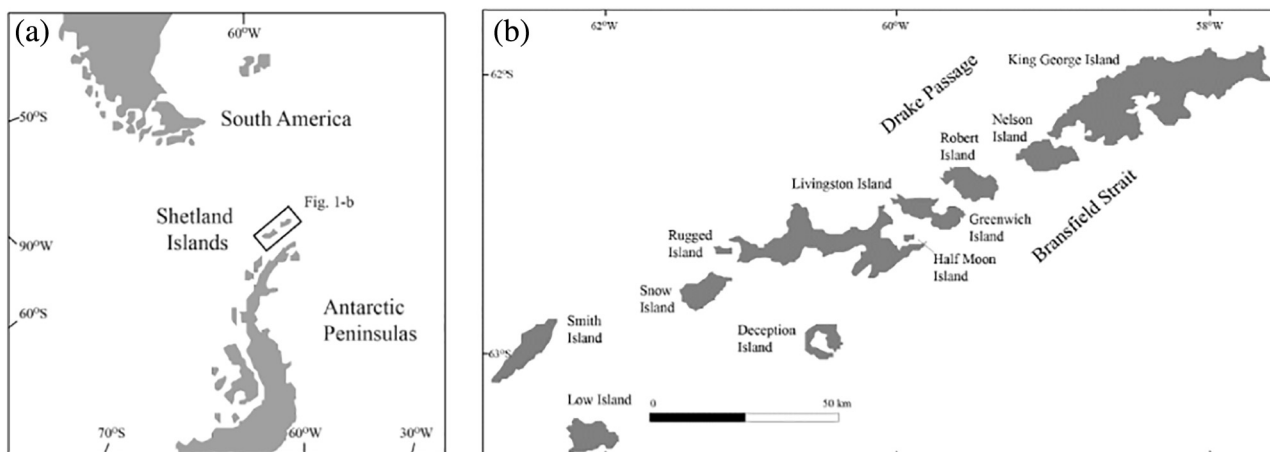


Fig. 1. Simplified map showing the location of (a) Shetland Islands and (b) Deception Island.

1994). Sulfate can therefore preserve isotopic information about its source and oxidation processes (Krouse and Mayer, 2000). Dissolved sulfate has been studied to understand global sulfur cycling and the role of atmospheric oxidants (e.g., O_3 , H_2O_2 , $\cdot OH$, O_2) (Krouse and Mayer, 2000; Bao, 2015).

SO_2 oxidation by atmospheric processes can be traced using anomalies of the $\Delta^{17}O_{\text{sulfate}}$ values (Savarino et al., 2000). The $\Delta^{17}O_{\text{sulfate}}$ anomalies in the sulfates have been studied for the atmospheric oxidation pathways from the dissolved sulfate in Antarctic ice cores (Alexander et al., 2002; Kunasek et al., 2010; Sofen et al., 2011), in Arctic sulfate aerosols (McCabe et al., 2006; Alexander et al., 2009), and for sea salt aerosol (Alexander et al., 2005; Dominguez et al., 2008).

Since sulfate from various sources shows different sulfur isotopic ratios (Nielsen, 1974; Rees et al., 1978; Calhoun et al., 1991; Krouse and Mayer, 2000), sulfur isotope values ($\delta^{34}S$) have been used to trace the source of dissolved sulfate (Patris et al., 2000; Otero et al., 2008; Tuttle et al., 2009; Lim et al., 2014) and aerosol sulfate (Guo et al., 2010; Chen et al., 2017), and the oxidation process of SO_2 by various atmospheric oxidants and their sulfur isotopic fractionation (Harris et al., 2012; Harris et al., 2013). Sulfur isotope anomalies ($\Delta^{33}S$ and $\Delta^{36}S$) of rare stable isotopes, such as ^{33}S and ^{36}S , have been used to identify mass-independent isotope fractionation processes in the present-day atmosphere, including photochemical oxidation reactions occurring in the stratosphere (Romero and Thiemens, 2003; Savarino et al., 2003; Baroni et al., 2008), and have been used to estimate mixing between stratospheric and tropospheric sources (Alexander et al., 2003; Pruett et al., 2004; Kunasek et al., 2010).

Oxygen and sulfur isotopes in sulfate in Antarctic ice cores (Patris et al., 2000; Alexander et al., 2002; Alexander et al., 2003; Pruett et al., 2004; Jonsell et al., 2005; Kunasek et al., 2010; Sofen et al., 2011) and in lakes and ponds (Sun et al., 2015) have been studied to understand the sources of sulfate and oxidation processes that lead to its generation. Anthropogenic sulfates are negligible in the Antarctic region (Patris et al., 2000; Alexander et al., 2003; Pruett et al., 2004; Kunasek et al., 2010), while elevated anthropogenic sulfate is seen in the Greenland ice core because of a relatively high level of human activities in the Northern Hemisphere (Patris et al., 2002). Surface and subsurface processes could modify an original isotopic signature of dissolved sulfate in water. The processes include (1) mixing of sulfate sources such as atmospheric sulfate, terrestrial sources and biological sulfate (Krouse and Mayer, 2000), (2) biological dissimilatory sulfate reduction, which results in significant fractionation (increase) of $\delta^{18}O$ and $\delta^{34}S$ in the residual sulfate (Nakai and Jensen, 1964; Fritz et al., 1989; Van Stempvoort and Krouse, 1994), and (3) oxidative weathering of sulfide, which brings about little sulfur isotope fractionation, but substantial oxygen isotope fractionation by kinetic isotope fractionation or isotopic

exchange with ambient water (Taylor et al., 1984; Van Stempvoort and Krouse, 1994; Balci et al., 2007).

Oxidative weathering processes occur in surface freshwater systems including lakes, ponds, rivers and groundwater (Otero et al., 2008; Rock and Mayer, 2009; Yuan and Mayer, 2012). The oxidation process of sulfide to sulfate proceeds by $Fe(III)_{aq}$ or O_2 as oxidants with ambient water (Balci et al., 2007 and references therein). This source contrasts with the source of ice-core sulfate where atmospheric deposition is the dominant process without the effect of surface and subsurface processes (Patris et al., 2000; Alexander et al., 2003). Recent isotope analysis in sulfate from glaciogenic deposits within the central Transantarctic Mountains show extremely high $\delta^{34}S$ values (up to 50‰) of mirabilite, which reflect dissimilatory microbial sulfate reduction (Sun et al., 2015). Sun et al. (2015) reported exceptionally low $\delta^{18}O$ values (-22.2‰) and positive $\Delta^{17}O$ anomalies (up to 2.3‰) in the pond sulfate as well.

The dissolved sulfate in lakes, ponds, and creeks has various channels of sulfate supply compared to the ice core supply, which includes only atmospheric deposition (Sun et al., 2015). Considering the small influx of anthropogenic sulfate in Antarctica (Patris et al., 2000), sulfates dissolved in the Antarctic surface water could provide an important perspective on sulfate formation, transportation, atmospheric and surface oxidation processes, and even biological processes in the Antarctic region. Here we report the ion concentrations (Na^+ , Ca^{2+} , SO_4^{2-} , Cl^-) and the multiple oxygen ($\delta^{18}O$ and $\Delta^{17}O$) and sulfur ($\delta^{34}S$, $\Delta^{33}S$ and $\Delta^{36}S$) isotope ratios of the dissolved sulfates in freshwater from the lakes, ponds, and creeks of Deception Island, a caldera island located in the Antarctic Peninsula. We (1) examine the effect of evaporation, mixing and biological processes on sulfate concentration and isotopic composition, (2) identify the sources of dissolved sulfate and their respective contributions, (3) estimate the oxidation pathway of SO_2 to form sulfate in the atmosphere and the relative fraction of atmospheric oxidants using the oxygen isotopic compositions ($\Delta^{17}O$ and $\delta^{18}O$) of sulfates, and (4) discuss the implication and significance of both the $\Delta^{33}S$ and $\Delta^{36}S$ values in the dissolved sulfate.

2. Geological background

The South Shetland Islands are located at the Antarctic Peninsular side in the Drake Passage (Fig. 1a), formed by the subduction of the former Phoenix Plate in the Mesozoic and Cenozoic (Machado et al., 2005). Volcanic activity occurring in the late Jurassic and early Cretaceous was related to this subduction, leading to the formation of the Antarctic Peninsula including the South Shetland Islands in the Mesozoic and Cenozoic (Machado et al., 2005). The South Shetland Islands are a calc-alkaline island arc formed during the Jurassic and Tertiary and show a typical subduction-related component including pyroclastic

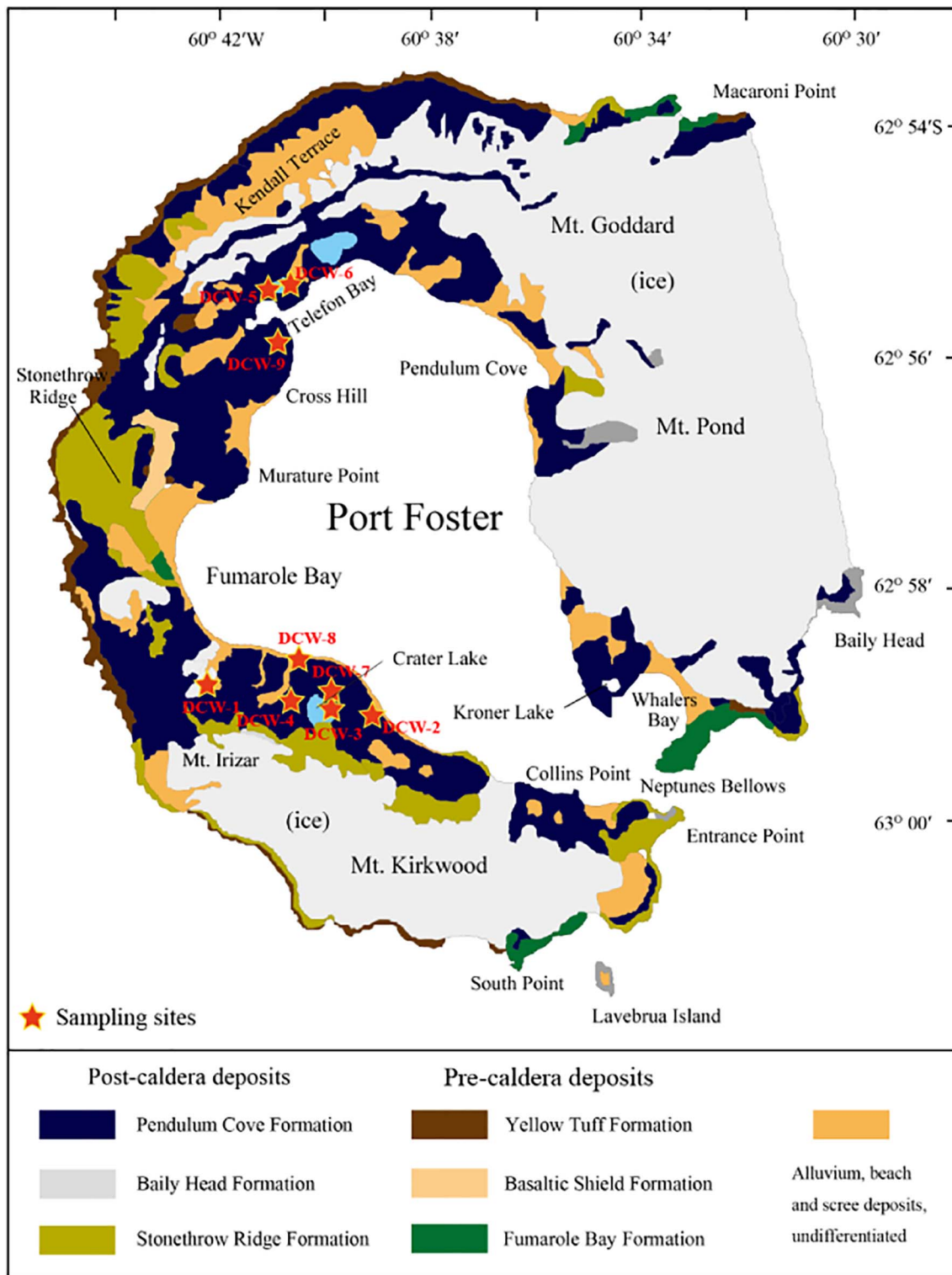


Fig. 2. Geological map of Deception Island (modified from Smellie and López-Martínez, 2000) and sampling locations of ponds and lakes.

deposits, mafic to felsic plutons and intrusive bodies (Smellie et al., 1984; Machado et al., 2005; Lee et al., 2008).

Deception Island, located in the SW of the South Shetland Islands, is an active Quaternary volcanic caldera (Fig. 1b) with the latest eruption recorded in 1970. The collapsed central part of the caldera (Port Foster) makes the island ring- or horseshoe-shaped as shown in Fig. 2 (Baraldo and Rinaldi, 2000). This large (8–10 km in diameter) caldera formed from summit collapse associated with small effusive and pyroclastic

eruptions (Baker et al., 1975; Smellie et al., 1984; Smellie, 2001). The composition of erupted volcanic rocks in Deception Island varies from basalt to dacite (Weaver et al., 1979; Smellie, 2001). More evolved volcanic rocks with andesitic composition occur in the tuff cones within the caldera (Smellie, 2001).

The volcanic rock units of Deception Island are stratigraphically divided into pre-caldera deposits and post-caldera deposits (Baker et al., 1975; Baraldo and Rinaldi, 2000). The pre-caldera deposits are

subdivided into the Fumarole Bay Formation (FBF), Basaltic Shield Formation (BSF) and Yellow Tuff Formation (YTF) (Smellie, 2001). The FBF is the oldest pre-caldera unit including a thick succession of massive basaltic breccia, fine lapilli stone and coarse lapilli tuff (Smellie, 2001). The BSF consists of sheet lava flows and scoria deposits (Smellie, 2001). The YTF is the most widespread unit in Deception Island (Smellie, 2001). The YTF is mainly composed of the palagonitized yellowish lapilli tuffs and unconformably overlies the FBF and BSF (Smellie, 2001). The YTF is also called the Outer Coast tuff Formation because of its conspicuous occurrence in the outer coast cliffs of Deception Island (Fig. 2).

Smellie (2001) recently divided the post-caldera deposits further into the Stonethrow Ridge Formation (SRF), Baily Head Formation (BHF) and Pendulum Cove Formation (PCF). The post-caldera deposit is unconformably in contact with the pre-caldera deposit at its lower boundary (Smellie, 2001). The SRF is composed of basalt, andesite, scoria and lavas, and is located in the outer slopes of Deception Island (Smellie, 2001). The lapilli stones and tuffs are dominated in the BHF, showing an unconformity on mainly the SRF (Smellie, 2001). The PCF includes the lapilli tuffs and ashes forming the surface outcrop of Deception Island (Smellie, 2001).

3. Water sampling, preparation, and analytical techniques

A total of 9 freshwater samples were collected at Deception Island in 2006 for isotope analysis in the dissolved sulfates and ion analysis (Figs. 2 and 3). In all, 6 samples were from the crater lakes, 2 from the unnamed ponds, and 1 from a creek “the Mekong River” (Table 1). The sampling sites are described in Table 1. More than 40 l of water was sampled from each site. Some field photos of representative sampling sites are shown in Fig. 3.

We used anion exchange resin (Amberlite IRA 400) columns (Hong and Kim, 2005) to pre-concentrate the dissolved sulfates at the Antarctic base. A total of 36 l of water was adjusted to pH 3–4 by adding a 10% HCl solution. The water samples were subsequently passed through a 0.45 µm water filter to remove particles and the anion exchange column at a flow rate of < 4 l per hour.

The collected sulfates in the columns were eluted using NaCl-rich water in the laboratory at the Seoul National University, and 10% BaCl₂ solution was added to the eluted solution to precipitate BaSO₄ after adjusting the pH to 3–4 by using concentrated HCl. The precipitated BaSO₄ was filtered and dried for the isotope analysis. Water samples for the major ion analysis were not chemically pre-treated.

Ca²⁺ and Na⁺ in the water were determined using an inductively coupled plasma-atomic emission spectrometer (ICP-AES: Optima-4300DV) at the National Center for Inter-university Research facilities, and anions such as Cl⁻, SO₄²⁻ and NO₃⁻ were determined by an ion chromatography (IC) system (Dionex/ICS-3000) at the National Instrumentation Center for Environmental Management in the Seoul National University. The detection limits of major anions by the IC system, and Na⁺ and Ca²⁺ by ICP-AES are 1, 0.05 and 0.01 mg/L, respectively.

For sulfur isotope analysis, the precipitated BaSO₄ powder was converted into gaseous H₂S using the THODE reduction solution of HI + H₃PO₂ + HCl (Thode et al., 1961) and the H₂S was bubbled into a AgNO₃ solution by N₂ as a carrying gas. Silver sulfide was precipitated and stored in a dark room for a week for stabilization. The silver sulfide was centrifuged, the silver nitrate solution decanted off, and the silver sulfide was then washed with a succession of Milli-Q (MQ) water rinses, followed by a rinse with 20 ml of 1 M NH₄OH and then several additional MQ water rinses. A total of 3 mg of dried Ag₂S was weighed into an aluminum foil package and reacted with a 10-fold excess of elemental fluorine in a nickel vessel for 8 h at 250 °C. The sulfur hexafluoride (SF₆) thus produced was separated from F₂ by a liquid nitrogen trap and purified from HF by an ethanol slush at -110 °C. The fluorine gas was passivated using KBr (potassium bromide) salt and the distilled

SF₆ then moved into the injection loop of a gas chromatograph (GC). The final procedure was carried out using a GC-TCD with a column composed of a 1/8 in. diameter and 6 ft length column including type 5A sieve and a second 1/8 in. diameter and 12 ft length HayeSep-Q™ column. The SF₆ was eluted from the column by the helium gas and a spiral trap froze the sulfur hexafluoride from the He using liquid nitrogen.

Multiple sulfur isotope compositions were determined by using a Thermo-Finnigan Mat 253 Dual Inlet Isotope Ratio Mass Spectrometer at the University of Maryland. The δ notation was used to represent δ³⁴S values relative to VCDT reference using the following equations:

$$\delta^{34}\text{S} = 1000 \times ((^{34}\text{S}/^{32}\text{S}_{\text{sample}}) - (^{34}\text{S}/^{32}\text{S}_{\text{reference}})) / (^{34}\text{S}/^{32}\text{S}_{\text{reference}}) \quad (1)$$

Δ³³S and Δ³⁶S were calculated by the equations below (Farquhar et al., 2000):

$$\Delta^{33}\text{S} = \delta^{33}\text{S} - 1000 \times ((1 + \delta^{34}\text{S}/1000)^{0.515} - 1) \quad (2)$$

$$\Delta^{36}\text{S} = \delta^{36}\text{S} - 1000 \times ((1 + \delta^{34}\text{S}/1000)^{1.90} - 1) \quad (3)$$

The uncertainties of δ³⁴S, Δ³³S and Δ³⁶S are 0.20‰, 0.008‰ and 0.16‰ respectively, estimated on the long-term measurements of standard materials (IAEA S-1).

Multiple oxygen isotope compositions (¹⁶O, ¹⁷O and ¹⁸O) of sulfate were determined by using a CO₂-laser fluorination system (Bao and Thiemens, 2000). The precipitated BaSO₄ powder was further purified using the DDARP method (Bao, 2006) to remove nitrate. The purified BaSO₄ then was analyzed for ¹⁸O/¹⁶O ratios by converting BaSO₄ to CO through a Thermal Conversion Elemental Analyzer (TCEA) at 1450 °C, and for ¹⁷O/¹⁶O ratios by converting BaSO₄ to O₂ using a CO₂-laser fluorination system (Bao and Thiemens, 2000). The ¹⁸O/¹⁶O ratios were run in continuous-flow mode, whereas the ¹⁷O/¹⁶O ratios were run in dual-inlet mode. Both were run on a MAT 253 at Louisiana State University. The analytical standard deviation (1 sigma) for replicate analysis associated with Δ¹⁷O and δ¹⁸O is 0.05‰ and 0.5‰, respectively.

Oxygen isotope compositions of sulfate samples were presented by δ-notation relative to SMOW (Standard Mean Ocean Water) values as followed:

$$\delta^{18}\text{O} = 1000 \times ((^{18}\text{O}/^{16}\text{O}_{\text{sample}}) - (^{18}\text{O}/^{16}\text{O}_{\text{reference}})) / (^{18}\text{O}/^{16}\text{O}_{\text{reference}}) \quad (4)$$

The Δ¹⁷O anomalies were calculated using the following equation:

$$\Delta^{17}\text{O} = \delta^{17}\text{O} - 0.52 \times \delta^{18}\text{O} \quad (5)$$

4. Results

The δ³⁴S_{sulfate} values for Deception Island water samples range from 8.1‰ to 17.3‰, and the Δ³³S_{sulfate} and Δ³⁶S_{sulfate} values range from 0.00‰ to 0.05‰ and from -0.26‰ to 0.01‰, respectively (Table 2). The analyzed δ¹⁸O_{sulfate} values are from -4.6‰ to 0.7‰, and Δ¹⁷O_{sulfate} are from -0.22‰ to -0.01‰ (Table 2). The concentrations of Ca²⁺, Cl⁻, and SO₄²⁻ ions in the water were from 0.7 mg/L to 16.0 mg/L, from 9.2 mg/L to 310 mg/L, and from 1.2 mg/L to 84.0 mg/L, respectively (Table 2). The samples from the lakes (DCW-2 and DCW-3) with lower values of δ³⁴S_{sulfate}, i.e., 9.2‰ and 8.1‰ showed higher SO₄²⁻, Ca²⁺ and Cl⁻ concentrations relative to other samples. The concentrations of NO₃⁻ ions were determined to be below the detection limit (1 mg/L) (Table 2).

5. Discussion

The potential sources and formation processes of the dissolved sulfates in the freshwater in the Antarctic region can be constrained by using its sulfur and oxygen isotopic compositions and major ion concentrations of the Deception Island water.

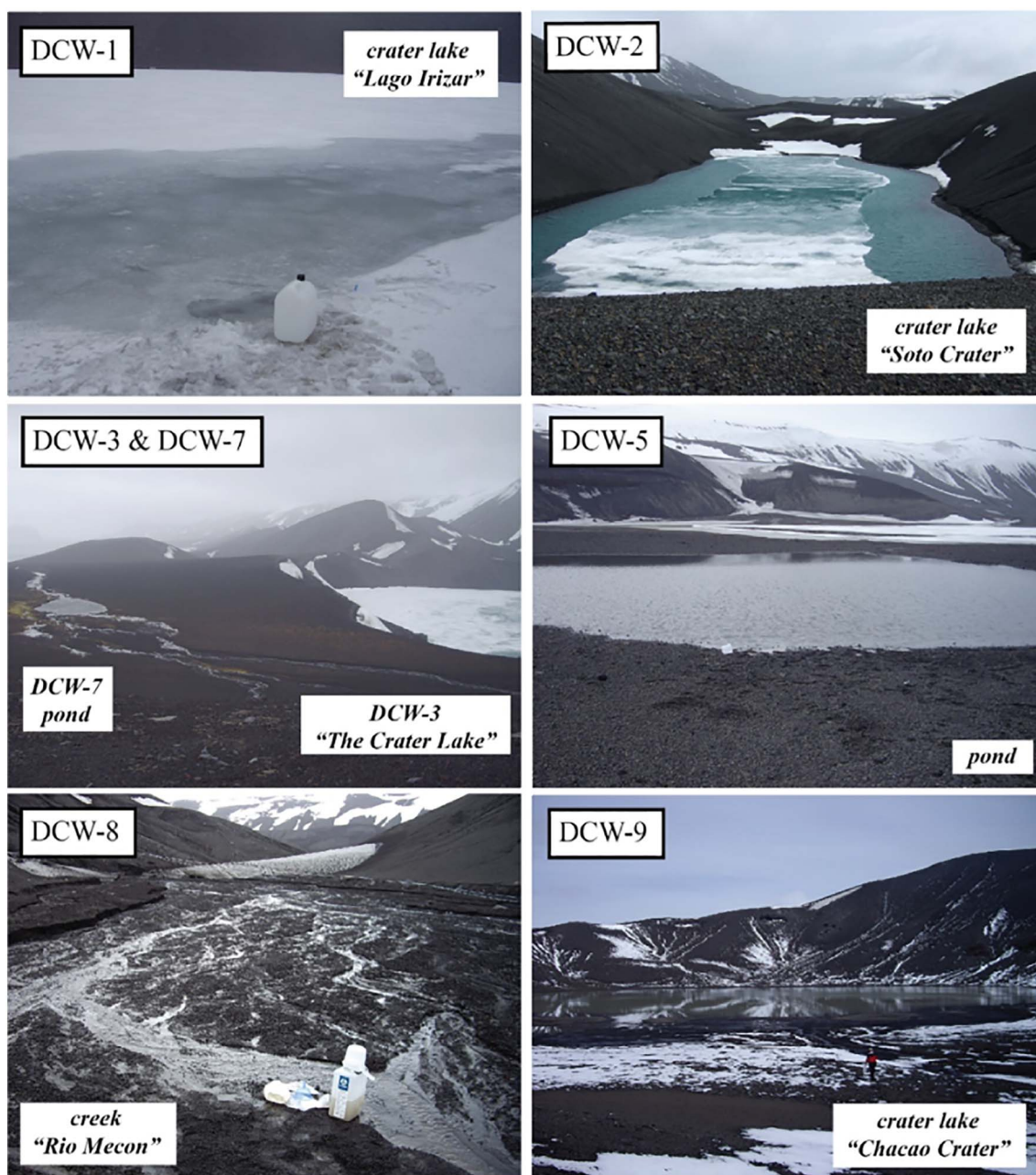


Fig. 3. Photos of representative sites for surface water collection.

Table 1

Description of water sampling sites at the Deception Island.

Sample	Name	Description	Latitude	Longitude	elevation
DCW-1	Crater lake "Lago Irizar"	Crater lake surrounded by volcanic pyroclasts. Surface was frozen.	62°58'49.3"S	60°42'23.9"W	4.0 m
DCW-2	Crater lake "Soto Crater"	Crater lake surrounded by volcanic pyroclasts. Surface in the central part of the lake was frozen.	62°59'05.2"S	60°39'16.9"W	1.5 m
DCW-3	Crater lake, "the Crater Lake"	Biggest crater lake near the Spanish Antarctic base. Crater lake surrounded by volcanic pyroclasts and lava flow. Surface was frozen.	62°58'57.6"S	60°40'01.1"W	< 1.0 m
DCW-4	Crater lake "Crater Zapatilla (Shoes lake)"	Lake near DCW-3 site and the Spanish Antarctic base	62°58'59.3"S	60°40'35.9"W	Not determined
DCW-5	Pond, name unknown	Shallow pond	62°55'29.1"S	60°40'56.7"W	8.2 m
DCW-6	Crater lake, name unknown	Crater lake with muddy water	62°55'26.1"S	60°40'52.2"W	2.8 m
DCW-7	Pond, name unknown	Pond with lichen and moss nearby. Steam from geothermal activity. Waters coming from melting of nearby ice	62°58'51.5"S	60°39'55.5"W	20.9 m
DCW-8	"Rio Mecon" (Mekong River)	Muddy creek. Water from melting of nearby glacier	62°58'37.7"S	60°40'39.2"W	Not determined
DCW-9	Crater lake, "Chacao Crater"	Crater lake surrounded by volcanic pyroclasts. Muddy water	62°56'00.0"S	60°40'55.7"W	Not determined

Table 2
Isotopic composition of the dissolved sulfate and major ion concentrations of water from Deception Island. Calculated sea salt fraction (F) and the calculated S isotopic composition of non-sea salt sulfate (nss). Oxygen and hydrogen isotope ratios in the water (Kusakabe et al., 2009). The entry “nd” represents “not determined”.

	$\Delta^{34}\text{S}_{\text{sulfate}}$ (‰)	$\Delta^{33}\text{S}_{\text{sulfate}}$ (‰)	$\Delta^{36}\text{S}_{\text{sulfate}}$ (‰)	$\delta^{18}\text{O}_{\text{sulfate}}$ (‰)	$\Delta^{17}\text{O}_{\text{sulfate}}$ (‰)	Cl ⁻ (mg/L)	SO ₄ ²⁻ (mg/L)	NO ₃ ⁻ (mg/L)	Ca ²⁺ (mg/L)	Na ⁺ (mg/L)	³⁴ S (sea salt fraction)	nss- $\delta^{34}\text{S}_{\text{sulfate}}$ (‰)	δD (‰)	$\delta^{18}\text{O}$ (‰)
DCW-1	17.2	0.05	0.01	0.7	-0.11	37	6.0	nd	0.7	23.0	0.27	15.8	-64.2	-8.6
DCW-2	9.2	0.00	0.19	-4.6	-0.22	310	84.0	nd	16	210.0	0.18	6.6	-76.7	-10.5
DCW-3	8.1	0.00	-0.08	-2.7	-0.12	52	17.0	nd	2.8	40.0	0.16	5.6	-75.9	-10.0
DCW-4	15.5	0.01	-0.14	-0.1	-0.08	9.2	1.2	nd	0.9	6.3	0.36	12.3	-80.9	-10.9
DCW-5	17.3	0.04	-0.09	-2.0	-0.10	22	3.4	nd	1.3	14.0	0.28	15.9	-63.9	-7.8
DCW-6	16.9	0.03	-0.26	-1.2	-0.07	20	2.8	nd	1.6	12.0	0.29	15.1	-81.9	-10.9
DCW-7	17.1	0.03	-0.2	-3.6	-0.10	17	2.3	nd	1.7	14.0	0.43	14.2	-71.5	-9.9
DCW-8	15.2	0.02	-0.19	-0.3	-0.01	nd	nd	nd	5.5	0.5	nd	nd	-80.0	-10.8
DCW-9	16.0	0.04	-0.11	-3.9	-0.09	26	4.0	nd	1.7	15.0	0.27	14.2	-76.0	-10.0

^a Sea salt fraction calculated by $k = 0.07$.

^b From Kusakabe et al. (2009).

5.1. Calculation of non-sea salt sulfate

The contribution of sea salt sulfate to total sulfate can be estimated from sodium ion (Na⁺) and sulfate ion (SO₄²⁻) concentration. We evaluated the sea-salt fraction (F) by the following equation,

$$F = k[\text{Na}^+]_{\text{measured}}/[\text{SO}_4^{2-}]_{\text{measured}} \quad (6)$$

where k is the $[\text{SO}_4^{2-}]/[\text{Na}^+]$ mass concentration ratio of SO₄²⁻ and Na⁺ in the sea salt. The k value of the open ocean is 0.25 (Holland, 1978). The sea salt fraction (F) of Deception Island water in this study calculated using $k = 0.25$ is > 1 , thus resulting in a negative estimation of non-sea salt (nss) sulfate concentration. The overestimation of the F value calculated by using $k = 0.25$ has been reported and discussed for the ice samples near the Antarctic coastal regions (Minikin et al., 1994; Wagenbach et al., 1998; Rankin et al., 2000; Jonsell et al., 2005; Kunasek et al., 2010).

Rankin et al. (2000) argued that the k value could possibly be lower than 0.25 in the Antarctic region due to the formation of frost flowers in the polar ocean. Frost flowers are saline and fragile ice crystals generated from the highly saline brine on the sea ice (Nghiem et al., 1997). This saline brine is formed by the sea salt expelled from the low-saline ice as seawater is frozen (Richardson, 1976; Perovich and Richter-Menge, 1994). As the temperature falls the brine-to-ice volume ratio decreases and this makes the brine more saline, giving rise to salt precipitation (Rankin et al., 2000). The precipitation of mirabilite (Na₂SO₄·10H₂O) begins below -8°C and the incorporation of the precipitates into the sea ice under the brine leads to surface brine depleted in both sodium and sulfate (Rankin et al., 2000). The measurements of ion concentrations in frost flowers showed the substantial fractionation among sea-salt ions (Rankin et al., 2000). They discussed that sulfate ion concentration of frost flowers decreased to 10.8% of the seawater concentration, which is three times lower than the decrease in other major ions, such as K⁺ (36.4%), Mg²⁺ (38.1%), Ca²⁺ (39.4%) and Cl⁻ (35.2%). In contrast, sodium ion concentration was reduced to 33.8% of the seawater concentration, which was approximately 10% lower than other ions. The measured SO₄²⁻-to-Na⁺ ratio of frost flowers is 0.09, consistent with the mirabilite lost from the surface brine to submerged ice (Rankin et al., 2000). The estimated k values which that been reported from the coastal Antarctic region were 0.07 (Wagenbach et al., 1998; Kunasek et al., 2010) and 0.09 (Rankin et al., 2000; Jonsell et al., 2005).

By assuming the strong influence of frost flowers contributed to the total sea-salt concentration in the region, we applied the lowest estimated k value of 0.07 to the non-sea-salt sulfate calculation of Deception Island water. Deception Island is in the South Shetland Islands, part of the wide coastal area of the Antarctic Peninsula (Fig. 1). Since the frost flowers can be generated more in the coastal region compared to the open ocean water (Rankin et al., 2000; Kunasek et al., 2010), Deception Island would be easily affected by the frost flower production, which allows a significant amount of fractionated sea-salt aerosols including sulfates into the freshwater in the region. This could affect the concentration of Na⁺ and SO₄²⁻, and the sea salt fraction (F) of Deception Island water.

To eliminate the contribution from the sea-salt sulfate, the sulfur isotope value of non-sea-salt sulfate ($\delta^{34}\text{S}_{\text{nss}}$) was calculated by the following equation,

$$\delta^{34}\text{S}_{\text{nss}} = \frac{\delta^{34}\text{S}_{\text{measure}} - F \times \delta^{34}\text{S}_{\text{seawater}}}{(1 - F)} \quad (7)$$

where F is the fraction of sea salt calculated by Eq. (6) and $\delta^{34}\text{S}_{\text{seawater}}$ is the sulfur isotope value of seawater, 21‰ (Rees et al., 1978). While the calculated sea-salt fractions in this study are from 0.16 to 0.43 with an average of 0.28, the average $\delta^{34}\text{S}_{\text{nss}}$ value of the dissolved sulfate is 12.5‰ ranging from 5.6‰ to 15.9‰ by eliminating the sea-salt fraction (Table 2).

The sea-salt fractions and related $\delta^{34}\text{S}_{\text{nss}}$ values are calculated on the

assumption that most Na^+ in the water bodies originates from sea salt. In contrast to the Antarctic ice cores where most ions are derived from atmospheric deposition (e.g., Patris et al., 2000), the major ions including Na^+ , Ca^{2+} , Cl^- and SO_4^{2-} of the water bodies at the surface can originate from not only atmospheric deposition but also from the weathering process of volcanic rocks. The additional input of Na^+ into the water bodies can cause the overestimation of sea-salt fractions, and the underestimation of non-sea-salt sulfate and the $\delta^{34}\text{S}_{\text{nss}}$ value. Since Deception Island is composed of volcanic rock (Fig. 2), there is a possibility that weathering of the volcanic rock could supply additional Na^+ ions which are not associated with Cl^- and SO_4^{2-} into the water bodies. In this case, the calculated sea-salt fractions and the decrease of $\delta^{34}\text{S}_{\text{nss}}$ values from $\delta^{34}\text{S}$ might be smaller.

5.2. Sulfate from atmospheric deposition

In this study, we discuss the possible source of sulfates derived from the air. Atmospheric sulfate can be formed by natural processes such as volcanic eruption, sea salt, biogenic hydrogen sulfide and its oxidation products, DMS and its oxidation products, and mineral dust (Nielsen, 1974; Calhoun et al., 1991; Krouse and Mayer, 2000). Atmospheric sulfate can also be generated by anthropogenic activities such as fossil-fuel burning, fertilizer usage, and sewage (Krouse and Mayer, 2000; Bao and Reheis, 2003; Norman et al., 2004; Oduro et al., 2012; Amrani et al., 2013).

5.2.1. Sulfur isotopic signatures of sulfate from atmospheric deposition

5.2.1.1. Sulfate from terrigenous sources (volcanoes and mineral dust). Approximately 31 active volcanoes are located in the Antarctic region including the Antarctic Peninsula (Delmas et al., 1985; Jonsell et al., 2005). The SO_2 degassed from the active volcanoes and its oxidized product sulfate (volcanic sulfate) can be a candidate for a low $\delta^{34}\text{S}$ -bearing source. The $\delta^{34}\text{S}$ of the volcanic sulfate range from 0‰ to 5‰ (Nielsen, 1974; Calhoun et al., 1991). Volcanic sulfate has been considered as one of the non-sea-salt sulfate sources in Antarctic ice and snow samples (Patris et al., 2000; Alexander et al., 2003; Pruetz et al., 2004; Jonsell et al., 2005; Kunasek et al., 2010). Patris et al. (2000) estimated the y-intercept value of 2.8‰ in the plot of $\delta^{34}\text{S}_{\text{sulfate}}$ and $1/[\text{SO}_4^{2-}]$ from ice-core samples near the South Pole and suggested that the y-intercept with a low $\delta^{34}\text{S}_{\text{sulfate}}$ represents a volcanic sulfate end-member. While the relative contribution of volcanic sulfate varied from < 5% (Patris et al., 2000) up to 70% (Kunasek et al., 2010), the studies demonstrated that volcanic sulfate is a significant sulfate source in the snow, ice, and possibly water samples in the Antarctic region.

The y-intercept values of Deception Island water in the plots of $\text{Cl}^-/\text{SO}_4^{2-}$ molar ratio versus $\delta^{34}\text{S}_{\text{sulfate}}$ (Fig. 4a) and $\delta^{34}\text{S}_{\text{nss}}$ (Fig. 4b) are

2.3‰ and -0.1 ‰, respectively. The values are similar to the y-intercept value estimated by Patris et al. (2000) and they are in the range of the $\delta^{34}\text{S}$ of the volcanic sulfate from 0‰ to 5‰ (Nielsen, 1974; Calhoun et al., 1991). Since the regression line in Fig. 4 represents a relatively high correlation (0.85 in Fig. 4a and 0.74 in Fig. 4b), the y-intercept could be estimated as the lower end-member of the mixing trend of Deception Island water (Fig. 4). Therefore, volcanic sulfate might represent one of the lower end-member sulfates of Deception Island water.

Another possible sulfate source for the low $\delta^{34}\text{S}_{\text{sulfate}}$ might be the mineral dust from the continent. Since Antarctica is ice covered, Patagonia is on the nearest continent for the introduction of mineral dust onto Deception Island (Fig. 1). The reported $\delta^{34}\text{S}$ of Patagonian volcanic rocks and sulfide minerals ranged from -2.8 ‰ to 4.2‰ (Jovic et al., 2011; Lanfranchini et al., 2013; Moreira and Fernández, 2015). The contribution of sulfate transported from Patagonia and Antarctic-derived sulfate from exposed-rock areas such as the Antarctic Peninsula and Northern Victoria Land is difficult to distinguish, because the range of sulfur isotope ratios of both volcanic and continental-derived sulfate closely overlap.

The Ca^{2+} concentration in ice core and snow samples has been considered as a conservative ion and used as a tracer for continental sulfates in Antarctica (Legrand et al., 1997; Kunasek et al., 2010) and Greenland (Patris et al., 2002). To calculate the contribution of sulfate from by continental-derived material, non-sea salt calcium concentration has to be determined by the following equation,

$$[\text{SO}_4^{2-}]_{\text{con}} = m[\text{Ca}^{2+}]_{\text{nss}} \quad (8)$$

where $[\text{SO}_4^{2-}]_{\text{con}}$ and m are the concentration of continental sulfate and average mass ratio of $\text{SO}_4^{2-}/\text{Ca}^{2+}$ (~ 0.18), representative of dust emission (Legrand et al., 1997) used in the previous studies (Patris et al., 2002; Kunasek et al., 2010). The non-sea-salt concentration of calcium ($[\text{Ca}^{2+}]_{\text{nss}}$) is calculated by the known calcium to sodium ratio of seawater (0.038) from Legrand et al. (1997). The estimated fraction of continental sulfate in eight samples from Deception Island calculated by Eq. (8) are < 10% except for DCW-1, which has a negative value for non-sea-salt calcium concentration (Table 3). These low calculated fractions (< 10%) of continental-derived sulfate to the total sulfate budget suggest a minor role of the lower end-members of the mixing line shown in Fig. 4.

Similar to the overestimation of Na^+ from the weathering process of volcanic rock on Deception Island, the addition of Ca^{2+} from the volcanic rock could result in the overestimation of the continental sulfate fraction. This could overestimate the fraction of continental sulfate (Table 3) even though the values are sufficiently low that their contribution to total sulfate seems insignificant, i.e., < 10%.

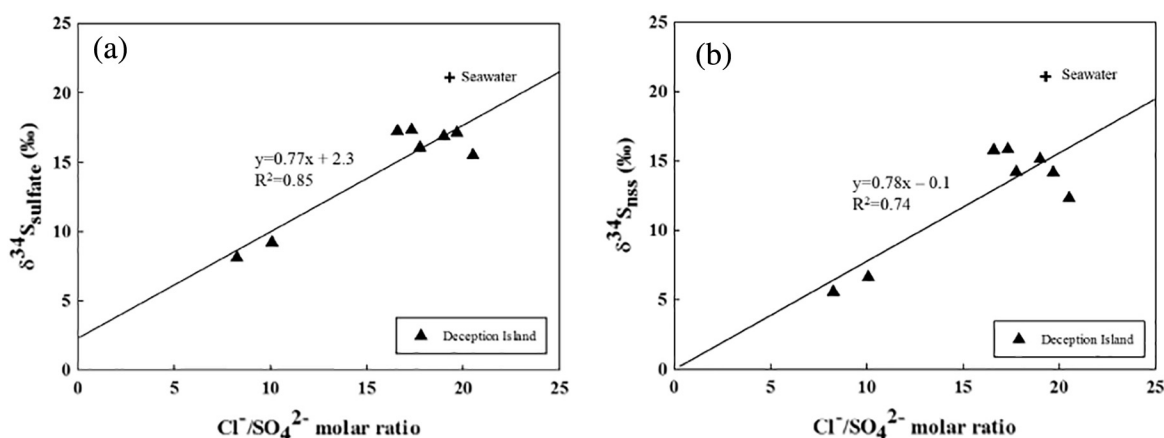


Fig. 4. Plots of $\text{Cl}^-/\text{SO}_4^{2-}$ molar ratio versus (a) $\delta^{34}\text{S}_{\text{sulfate}}$ and (b) $\delta^{34}\text{S}_{\text{nss}}$ values. The cross symbol indicates seawater. Both graphs show a linear regression line, the sign of the mixing line between two end-members. The y-intercepts, (a) 2.3 and (b) -0.1 , indicate the sulfur isotope values for lower end-member, which is volcanic sulfate from the constantly degassing volcanoes and/or mineral dust. The higher end-member sulfate consists of the combination of sea-salt aerosol and marine biogenic sources such as DMS.

Table 3

Calculated concentration of non-sea-salt calcium ion and sulfate ion from continental sources. The fraction of sulfate from continental source to total sulfate concentration was estimated. The entry “nd” represents “not determined”.

	Ca ²⁺ (mg/L)	a _{ns} Ca ²⁺ (mg/ L)	b _{ns} SO ₄ ²⁻ (mg/ L)	Fraction of continental sulfate (%)
DCW-1	0.7	−0.1 ^c	−0.03 ^c	−43 ^c
DCW-2	16	7.9	1.4	1.7
DCW-3	2.8	1.3	0.2	1.3
DCW-4	0.9	0.7	0.1	10.1
DCW-5	1.3	0.8	0.1	4.3
DCW-6	1.6	1.1	0.2	7.3
DCW-7	1.7	1.1	0.2	8.8
DCW-8	5.5	nd	nd	nd
DCW-9	1.7	1.1	0.2	5.0

^a Sea-salt fraction calculated by calcium to sodium mass ratio of seawater (0.038) from Legrand et al. (1997).

^b Calculated from average mass ratio of sulfate-to-calcium ratio of dust emission (0.18) suggested by Legrand et al. (1997).

^c The negative value might be attributed to the evaporation effect.

5.2.1.2. Sulfate from sea salt and marine biogenic sources. The end-member of the high sulfur isotope ratio could possibly be sea-salt aerosol and marine biogenic sources such as dimethyl sulfide (DMS) (Calhoun et al., 1991; Norman et al., 2004), or the combination of both (Fig. 4a). The $\delta^{34}\text{S}$ of seawater is 21‰ (Rees et al., 1978) and that of DMS and its oxidation products are from 16‰ to 19‰ (Oduro et al., 2012; Amrani et al., 2013). This range includes the $\delta^{34}\text{S}$ value of marine biogenic sulfate, +18.6‰, of the shallow Antarctic ice core near the South Pole (Patris et al., 2000). Fig. 4a and b show a similar trend, indicating that sulfate sources with high $\delta^{34}\text{S}$ values are associated not only with sea-salt sulfate but also with the supply of sulfate from marine biogenic sources, mainly DMS. Although ancient evaporite has a high sulfur isotope composition up to 35‰ as well (Krouse and Mayer, 2000), since Deception Island is mainly composed of Quaternary volcanic rocks (Fig. 2), we ruled out it as a possible candidate for the high $\delta^{34}\text{S}_{\text{sulfate}}$.

Marine biogenic sulfate such as DMS has been suggested as a significant source of sulfate in the Antarctic ice core (Patris et al., 2000; Alexander et al., 2003; Pruett et al., 2004; Jonsell et al., 2005; Kunasek et al., 2010), while its relative contributions in the ice core of West Antarctica (low $\delta^{34}\text{S}_{\text{sulfate}}$) and East Antarctica (high $\delta^{34}\text{S}_{\text{sulfate}}$) are different. The contribution of DMS can even be up to 90% of total sulfate in Antarctica (Patris et al., 2000). Fig. 4 shows that six Deception Island water samples still maintain their high sulfur isotope composition after excluding the sea-salt fraction. DMS therefore can contribute significantly to the high $\delta^{34}\text{S}_{\text{sulfate}}$ end-member of Deception Island water.

5.2.1.3. Sulfate from anthropogenic sources. Atmospheric sulfates from anthropogenic activities, mainly from fossil-fuel burning, showed relatively low $\delta^{34}\text{S}_{\text{sulfate}}$ values ranging from −3‰ to 9‰ (Krouse and Mayer, 2000). Patris et al. (2002) showed that the anthropogenic sulfate ($\delta^{34}\text{S}_{\text{sulfate}} = 3.0\text{‰}$) influenced the Greenland ice cores, and they also suggested that the $\delta^{34}\text{S}_{\text{sulfate}}$ of anthropogenic sulfate is distinct despite the change in the dominant source region. In contrast to Greenland, lying in the Northern Hemisphere where dense human and industrial activities occur, the Antarctic region has been regarded as relatively isolated from anthropogenic pollutants (Patris et al., 2000; Alexander et al., 2003; Pruett et al., 2004; Jonsell et al., 2005; Kunasek et al., 2010). Anthropogenic sulfate is generally emitted to the atmosphere with other pollutants such as nitrates, which are used as indicators in groundwater and river water for contaminants or discharges produced by human activities (Bottrell et al., 2008; Otero et al., 2008; Rock and Mayer, 2009; Tuttle et al., 2009; Hosono et al., 2011a; Hosono et al., 2011b). Nitrate concentrations in Deception

Island water are below the detection limit of 1 mg/l, which also supports the hypothesis of negligible anthropogenic sulfate contribution to Deception Island water.

5.2.2. Oxygen isotope compositions ($\delta^{18}\text{O}$ and $\Delta^{17}\text{O}$) of atmospheric sulfate

The oxygen atoms of atmospheric sulfate are generally controlled by the principal oxidants in the atmosphere such as ozone (O_3), hydrogen peroxide (H_2O_2), hydroxyl radical ($\cdot\text{OH}$) and oxygen molecules (O_2) (Thompson, 1992). As sulfur dioxide (SO_2) and other sulfur compounds are oxidized in the atmosphere, the isotopic signature of these oxidants is transferred to the sulfate ($\Delta^{17}\text{O}$ and $\delta^{18}\text{O}$) (Savarino et al., 2000). Since isotopic exchange occurs between H_2O and $\cdot\text{OH}$ in the atmosphere, the oxygen isotope ratio ($\delta^{18}\text{O}$) and its mass dependent affinity ($\Delta^{17}\text{O}$) in $\cdot\text{OH}$ is closely related to that of water vapor. Other oxidants, however, have much higher ($\delta^{18}\text{O}$) and anomalous ($\Delta^{17}\text{O}$) values such as from 95 to 125‰ and 20–35‰ in O_3 respectively (Johnston and Thiemens, 1997), and from 21.9–52.5‰ and 1–2‰ in H_2O_2 respectively (Savarino and Thiemens, 1999). More recently, Vicars and Savarino (2014) reported the $\delta^{18}\text{O}(\text{O}_3)_{\text{bulk}}$ and $\Delta^{17}\text{O}(\text{O}_3)_{\text{bulk}}$ values in both Grenoble city and the Atlantic Ocean, of which the average values are 111.4 and 26.2‰ and 114.8 and 25.9‰ respectively. The $\delta^{18}\text{O}$ in O_2 is 23.5‰, and $\Delta^{17}\text{O}$ is −0.34‰ (Barkan and Luz, 2005).

The $\delta^{18}\text{O}_{\text{sulfate}}$ in the Deception Island water (from −4.6‰ to 0.7‰; Fig. 5) is lower than typical values of atmospheric sulfate suggested by Krouse and Mayer (2000). Among the major oxidants in the atmosphere for sulfate formation mentioned above, $\cdot\text{OH}$ would be a major oxidant and contribute to the oxygen isotope composition of atmospheric sulfate in the study area. The contribution of $\cdot\text{OH}$, however, is < 40% on a global scale (Sofen et al., 2011; Alexander et al., 2012) and approximately 11% in the Antarctic region (Sofen et al., 2011). The low $\delta^{18}\text{O}_{\text{sulfate}}$ values we observe may reflect incorporation of other low $\delta^{18}\text{O}$ sulfate sources in the surface environment.

The $\Delta^{17}\text{O}_{\text{sulfate}}$ in this study is non-anomalous and ranges from −0.01‰ to −0.22‰ (Fig. 6). The near-zero $\Delta^{17}\text{O}_{\text{sulfate}}$ values in this study are distinct from the previous reports of highly positive $\Delta^{17}\text{O}_{\text{sulfate}}$ values in the Antarctic ice cores such as up to 4.8‰ in Vostok (Alexander et al., 2002), 4.1‰ in Dome C (Alexander et al., 2003) and 2.5‰ in the WAIS Divide (Kunasek et al., 2010) and in the dissolved sulfate of the Transantarctic Mountains up to 2.3‰ (Sun et al., 2015). These reports suggested that the anomalous $\Delta^{17}\text{O}_{\text{sulfate}}$ value originates from the atmospheric oxidation of SO_2 by H_2O_2 and O_3 . The non-anomalous $\Delta^{17}\text{O}_{\text{sulfate}}$ indicates little incorporation of the anomalous $\Delta^{17}\text{O}$ signature from O_3 and H_2O_2 during the oxidation process. SO_2 oxidation by O_3 in the troposphere would transfer a quarter of the $\Delta^{17}\text{O}$ signature from O_3 to sulfate, and the $\Delta^{17}\text{O}_{\text{sulfate}}$ would therefore be from 6.3–8.8‰ (Savarino et al., 2000). The H_2O_2 transfers half of its anomalous signature to sulfate, producing $\Delta^{17}\text{O}_{\text{sulfate}}$ of 0.5–1‰ (Savarino and Thiemens, 1999; Savarino et al., 2000). These have been considered to be the major oxidation mechanisms that produce anomalous mass-independent $\Delta^{17}\text{O}_{\text{sulfate}}$ in the Antarctic ice cores (Alexander et al., 2002; Kunasek et al., 2010; Sofen et al., 2011) and ponds in Antarctica (Sun et al., 2015). Oxidation of SO_2 by the $\cdot\text{OH}$ radical produces non-anomalous $\Delta^{17}\text{O}_{\text{sulfate}}$ except under some conditions in the dry Arctic region (Morin et al., 2007). Thus, the slightly negative and mass-dependent $\Delta^{17}\text{O}_{\text{sulfate}}$ of Deception Island water implies that the contribution of oxidants with high $\Delta^{17}\text{O}$ values such as O_3 and H_2O_2 to sulfate production in the atmosphere was negligible or sufficiently small that the measured $\Delta^{17}\text{O}_{\text{sulfate}}$ may originate from $\cdot\text{OH}$ and O_2 , rather than O_3 and H_2O_2 .

A halogen-bearing oxidant could cause the near zero $\Delta^{17}\text{O}$ value in the studied area. The $\Delta^{17}\text{O}$ value of sulfate formed by the heterogeneous oxidation process by HOCl or HOBr is 0‰ because these halogen-containing oxidants promote the hydrolysis of sulfur and do not transfer their oxygen atoms and positive $\Delta^{17}\text{O}$ value (50‰) to sulfate during the oxidation process (Fogelman et al., 1989; Troy and Margerum, 1991; Alexander et al., 2012). Heterogeneous oxidation is

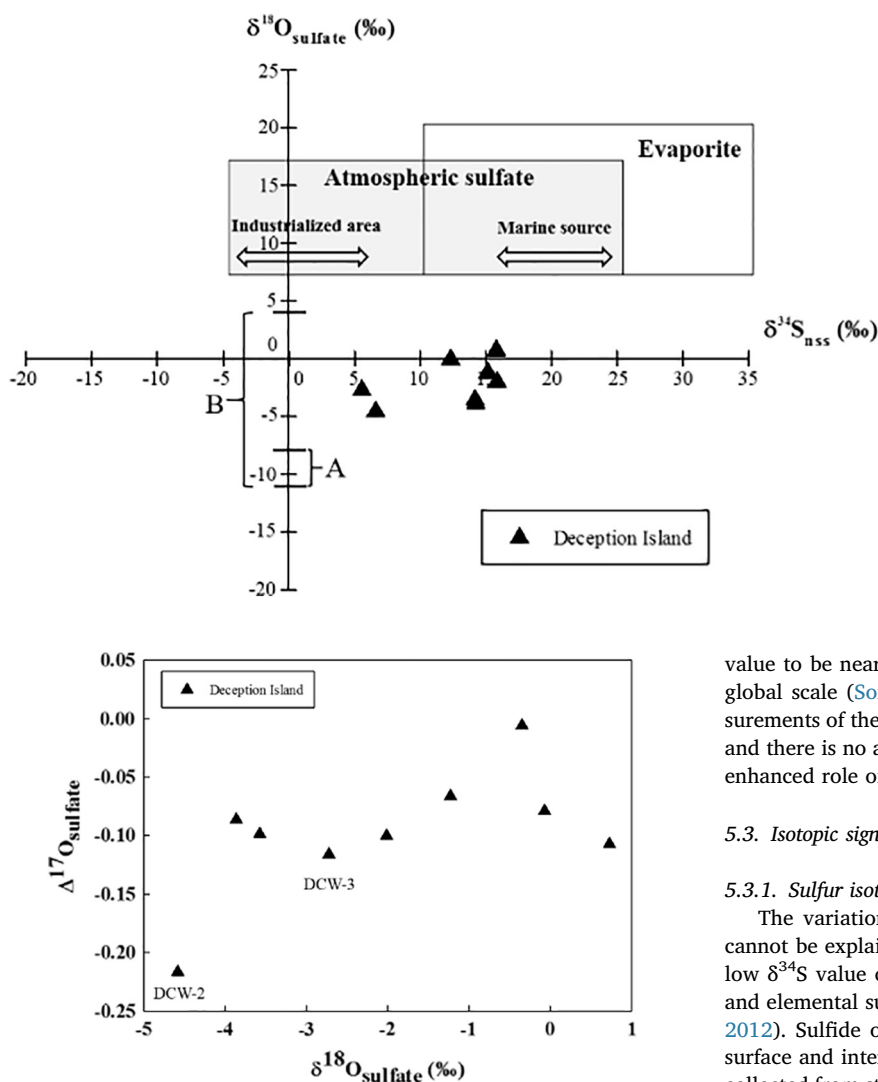


Fig. 6. Multiple oxygen isotope composition ($\Delta^{17}\text{O}$ and $\delta^{18}\text{O}$) of the dissolved sulfate from Deception Island. The $\Delta^{17}\text{O}_{\text{sulfate}}$ indicates no or little incorporation of mass-independent $\Delta^{17}\text{O}$ composition from O_3 and H_2O_2 during the atmospheric oxidation process. The non-anomalous $\Delta^{17}\text{O}_{\text{sulfate}}$ and lower $\delta^{18}\text{O}_{\text{sulfate}}$ than typical sulfate values imply the strong influence of the atmospheric $\cdot\text{OH}$ radical, which is isotopically representative of local ambient water. The slightly negative $\Delta^{17}\text{O}_{\text{sulfate}}$ implies the effect of O_2 , whose $\Delta^{17}\text{O}$ value was -0.23‰ , which in turn suggests an association with ambient water by the sulfide oxidation process.

thought to be especially important in the marine boundary layer (MBL) (Vogt et al., 1996) and model calculations indicate that it can contribute up to 30% of the total sulfate production in the atmosphere (von Glasow et al., 2002; Alexander et al., 2012). Heterogeneous oxidation by HOCl and HOBr on the surface of sea-salt aerosol can be enhanced when the concentration of the sea-salt aerosol increases and an alkaline condition (pH near 8) occurs in the MBL (Alexander et al., 2012). There is no evidence or direct measurement of high levels of halogen-containing oxidant in the studied area.

An association of $\cdot\text{OH}$ with the atmospheric oxidation process, which could explain the near zero $\Delta^{17}\text{O}_{\text{sulfate}}$ value in the study area, also lacks supporting evidence in spite of the zero $\Delta^{17}\text{O}$ value of $\cdot\text{OH}$ and the measured values of $\delta^{18}\text{O}_{\text{sulfate}}$, which are similar to the $\delta^{18}\text{O}_{\text{water}}$ in the water bodies of Deception Island. Partial involvement of $\cdot\text{OH}$ can contribute to the decrease of $\Delta^{17}\text{O}_{\text{sulfate}}$ values by both gas-phase and aqueous oxidation processes in the atmosphere (Jenkins and Bao, 2006). An anomalous increase in the $\cdot\text{OH}$ contribution to the overall atmospheric oxidation process of SO_2 can cause the $\Delta^{17}\text{O}_{\text{sulfate}}$

Fig. 5. Plot of the $\delta^{34}\text{S}$ versus $\delta^{18}\text{O}$ values of the dissolved sulfate from Deception Island. The areas of atmospheric sulfate and evaporite were from (Krouse and Mayer, 2000). The $\delta^{34}\text{S}_{\text{sulfate}}$ of the atmospheric sulfates in the industrialized area range from -3‰ to 9‰ (Krouse and Mayer, 2000), while the atmospheric sulfates derived from marine source such as sea-salt sulfate (21‰) (Rees et al., 1978), and marine biogenic sulfate (from 16‰ to 19‰) (Odoro et al., 2012; Amrani et al., 2013) show higher $\delta^{34}\text{S}_{\text{sulfate}}$. The letter A in the graph indicates the range of the $\delta^{18}\text{O}_{\text{water}}$ from Deception Island water (Kusakabe et al., 2009). The letter B in the graph means the estimated range of $\delta^{18}\text{O}_{\text{sulfate}}$ values produced from the sulfide oxidation process. The lower limit is the lowest $\delta^{18}\text{O}_{\text{water}}$ value of Deception Island water samples and the upper limit is calculated by the equation ($\delta^{18}\text{O}_{\text{sulfate}} = 0.62 * \delta^{18}\text{O}_{\text{water}} + 9$) from the experimental data suggested by Van Stempvoort and Krouse (1994). See the text for details.

value to be near zero since $< 40\%$ of sulfate is oxidized by $\cdot\text{OH}$ on a global scale (Sofen et al., 2011; Alexander et al., 2012). Direct measurements of the fractions of each oxidant in the atmosphere are absent and there is no adequate theoretical or simulation result to explain the enhanced role of $\cdot\text{OH}$ among major atmospheric oxidants.

5.3. Isotopic signatures of sulfate during the sulfide oxidation process

5.3.1. Sulfur isotopic composition during sulfide oxidation

The variation in the sulfur isotope value in the dissolved sulfate cannot be explained by only atmospheric contributions. Sulfate with a low $\delta^{34}\text{S}$ value can originate from the oxidation processes of reduced and elemental sulfur compounds (Tuttle et al., 2009; Yuan and Mayer, 2012). Sulfide oxidation could occur where sulfide is exposed at the surface and interacts with molecular oxygen. Sulfate in this study was collected from stagnant lake, pond, and creek water which came from a combination of precipitation, ice-melt and groundwater. Sulfate derived from sulfide mineral oxidation can be significant in surface waters (Otero et al., 2008; Rock and Mayer, 2009; Tuttle et al., 2009; Killingsworth and Bao, 2015) and in groundwater systems (Bottrell et al., 2008; Hosono et al., 2011b; Raidla et al., 2014). Since biological and abiotic oxidation of sulfides in the surface water leads to a relatively small fractionation of the sulfur isotope ratio of $< 2\text{‰}$ (Balci et al., 2007; Heidel et al., 2013), sulfate retains its original sulfur isotopic value.

The samples of two low $\delta^{34}\text{S}_{\text{nss}}$ (DCW-2 and DCW-3) and the other samples have a positive correlation between the $\delta^{34}\text{S}_{\text{nss}}$ and $\text{Cl}^-/\text{SO}_4^{2-}$ molar ratio (Fig. 4b). The lower $\delta^{34}\text{S}_{\text{nss}}$ samples are related to the increased sulfate concentration in the water. The two largest neighboring crater lakes (DCW-2 and DCW-3) are possibly the deepest among the water sampling sites of this study (Fig. 3). The water from these two lakes would have a relatively longer residence time and these would be better sites for an oxidative reaction of sulfide minerals, which could be an important candidate for the low $\delta^{34}\text{S}_{\text{sulfate}}$ and the elevated sulfate concentrations. Although the amount of sulfate derived from sulfide oxidation process may be small, the sulfur isotopic composition of total sulfate can be modified significantly due to the very low $\delta^{34}\text{S}$ value that may even be negative (Krouse and Mayer, 2000; Killingsworth and Bao, 2015).

5.3.2. Oxygen isotopic composition during sulfide oxidation

The $\delta^{18}\text{O}_{\text{sulfate}}$ could reveal the potential influence of the sulfide oxidation process on the total sulfate budget in surface water and

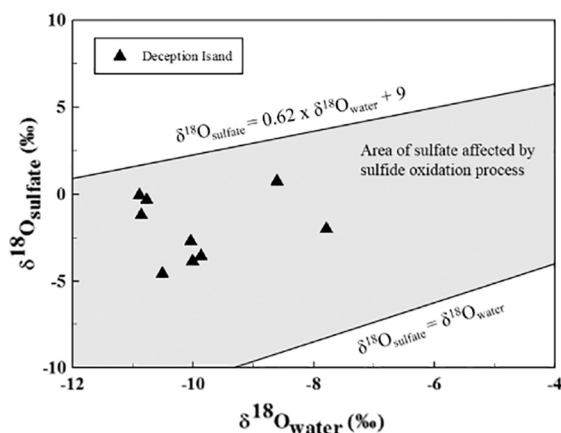


Fig. 7. Measured $\delta^{18}\text{O}_{\text{sulfate}}$ with $\delta^{18}\text{O}_{\text{water}}$ from Kusakabe et al. (2009). The shaded area defined by Van Stempvoort and Krouse (1994) indicates the field where the sulfate derived from sulfide oxidation has to be plotted in the $\delta^{18}\text{O}_{\text{sulfate}}$ vs. $\delta^{18}\text{O}_{\text{water}}$ diagram. The upper line ($\delta^{18}\text{O}_{\text{sulfate}} = \delta^{18}\text{O}_{\text{water}} * 0.62 + 9$) is the limit of $\delta^{18}\text{O}_{\text{sulfate}}$ values by the sulfide oxidation process with ambient water derived from the experimental data (Van Stempvoort and Krouse, 1994). The lower line ($\delta^{18}\text{O}_{\text{sulfate}} = \delta^{18}\text{O}_{\text{water}}$) means that no fractionation occurs between oxygen atoms during the oxidation process. The plot of sulfate samples of this study was located in the shaded area, implying a significant involvement of sulfate from the sulfide oxidation process.

groundwater (Krouse and Mayer, 2000; Otero et al., 2008; Yuan and Mayer, 2012). Since the oxygen atoms of the water molecule are incorporated into the sulfate during the sulfide oxidation process (Taylor et al., 1984; Van Stempvoort and Krouse, 1994; Balci et al., 2007), the $\delta^{18}\text{O}_{\text{sulfate}}$ could reflect the $\delta^{18}\text{O}_{\text{water}}$, representing the general relationship suggested by Van Stempvoort and Krouse (1994). Otero et al. (2008) argued that this relationship could be depicted as a field in the $\delta^{18}\text{O}_{\text{water}}$ and $\delta^{18}\text{O}_{\text{sulfate}}$ diagram and sulfates plotted in this area might indicate the significant influence of oxygen exchanged with water during the sulfide oxidation process. The lower limit of the field is represented by $\delta^{18}\text{O}_{\text{water}} = \delta^{18}\text{O}_{\text{sulfate}}$ indicating that all oxygen atoms of sulfate are derived from water molecule. The upper limit is defined as the equation of $\delta^{18}\text{O}_{\text{sulfate}} = 0.62 * \delta^{18}\text{O}_{\text{water}} + 9$, which is derived from experimental data (Van Stempvoort and Krouse, 1994). The samples of Deception Island water are plotted in this area (Fig. 7), suggesting a strong involvement of local water during the sulfide oxidation process. Although Deception Island water samples are plotted in the area, there seems to be no distinct relationship between the $\delta^{18}\text{O}_{\text{sulfate}}$ and $\delta^{18}\text{O}_{\text{water}}$ of Deception Island water samples (Fig. 7). This could be attributed to the fact that the sulfide oxidation process was not the only source for sulfate formation in Deception Island. Atmospheric sulfate might be one of the significant sulfate sources and the mixing process between the atmospheric sulfate and sulfate derived from sulfide oxidation process would prevent the $\delta^{18}\text{O}_{\text{sulfate}}$ from the sulfide oxidation process from preserving the signal of the $\delta^{18}\text{O}_{\text{water}}$ value.

The most negative reported $\delta^{18}\text{O}_{\text{sulfate}}$ value was -22.2‰ in the dissolved sulfate from the pond in the Transantarctic Mountains (Sun et al., 2015). Sun et al. (2015) suggested that this very low $\delta^{18}\text{O}$ value was affected by melting glacial water of which $\delta^{18}\text{O}$ became as low as -70‰ and that the calculated $\delta^{18}\text{O}_{\text{sulfate}}$ value from the weathering process was much lower than the previously reported value, down to -58.3‰ . The $\delta^{18}\text{O}_{\text{sulfate}}$ of Deception Island water, therefore, could be controlled by the oxygen isotopic composition of local water both in the atmosphere and at the surface.

Incorporation of sulfate from sulfide oxidation processes could explain the relatively lower $\delta^{18}\text{O}_{\text{sulfate}}$ of Deception Island water than typical atmospheric sulfate (Fig. 5). The association of water with the relatively lower $\delta^{18}\text{O}_{\text{water}}$, from -10.9‰ to -7.8‰ (represented as A in Fig. 5) can act as a medium for oxygen exchange during the process of sulfide oxidation. The maximum value of $\delta^{18}\text{O}_{\text{sulfate}}$ derived from the oxidation process was estimated as 4.1‰ determined by the equation

$\delta^{18}\text{O}_{\text{sulfate}} = 0.62 * \delta^{18}\text{O}_{\text{water}} + 9$ with the highest $\delta^{18}\text{O}_{\text{water}}$ (-7.8‰) of Deception Island water. The range of B is from -10.9‰ to 4.1‰ (Fig. 5) represents the estimated $\delta^{18}\text{O}_{\text{sulfate}}$ by the sulfide oxidation process with Deception Island water. This range includes the measured $\delta^{18}\text{O}_{\text{sulfate}}$ implying the influence of the local ambient water on the total sulfate budget of Deception Island water.

The slightly negative $\Delta^{17}\text{O}_{\text{sulfate}}$ (-0.22‰ to -0.01‰) may reflect the transfer of the $\Delta^{17}\text{O}$ signature of O_2 during the sulfide oxidation process. During the oxidation process at the surface, O_2 can be used as one of the major oxidants in addition to water molecules (Taylor et al., 1984; Van Stempvoort and Krouse, 1994; Balci et al., 2007). The negative $\Delta^{17}\text{O}$ of O_2 , -0.34‰ , would be transferred to sulfate and input of this sulfate to the total sulfate budget could make $\Delta^{17}\text{O}_{\text{sulfate}}$ negative within the mass-dependent fractionation range. Two samples (DCW-2 and DCW-3), which are considered to be more affected by the sulfide oxidation process than the other samples, represent the lowest $\Delta^{17}\text{O}_{\text{sulfate}}$ (-0.22‰ in DCW-2 and -0.12‰ in DCW-3; Table 2) of Deception Island water (Fig. 6). Since the fraction of O_2 as an atmospheric oxidant during oxidation to sulfate is $< 10\%$ (Alexander et al., 2012), the $\Delta^{17}\text{O}_{\text{sulfate}}$ transferred from $\Delta^{17}\text{O}_{\text{water}}$ via sulfide oxidation would be smaller than $\Delta^{17}\text{O}_{\text{water}}$ itself.

The incorporation of oxygen atoms from ambient water into sulfate and the partial involvement of the O_2 molecule depend on the sulfide oxidation reaction where the major oxidants are either O_2 or $\text{Fe(III)}_{\text{aq}}$ (Balci et al., 2007). The oxygen isotope ratios of sulfate incorporated from the O_2 molecule and water are varied by a related reaction pathway and can determine the $\delta^{18}\text{O}_{\text{sulfate}}$ value (Lloyd, 1968; Taylor et al., 1984; Balci et al., 2007). The negative $\Delta^{17}\text{O}$ value of the O_2 molecule (-0.34‰) might be further incorporated into the dissolved sulfate during the sulfide oxidation process when more O_2 molecules are involved in the reaction.

The $\delta^{18}\text{O}_{\text{sulfate}}$ value is expected to increase if more O_2 molecules are involved in the oxidation reaction due to its high $\delta^{18}\text{O}$ value (23.5‰). Several studies, however, showed that the oxygen isotope fractionation occurs during the sulfide oxidation reaction by the O_2 molecule and water, and this process might reduce the effect of its high $\delta^{18}\text{O}$ value on the sulfate (Lloyd, 1968; Taylor et al., 1984; Van Stempvoort and Krouse, 1994). The oxygen isotope fractionation between sulfate and the O_2 molecule reduces the $\delta^{18}\text{O}_{\text{sulfate}}$ to -11.4‰ while the reaction by the $\text{Fe(III)}_{\text{aq}}$ shows less variable isotope fractionation, 0‰ to 4‰ , between sulfate and water molecules (Lloyd, 1968; Taylor et al., 1984; Van Stempvoort and Krouse, 1994). This indicates that the high $\delta^{18}\text{O}$ value of the O_2 molecule is not fully reflected in the $\delta^{18}\text{O}_{\text{sulfate}}$ during sulfate formation by the sulfide oxidation process.

In the water bodies in oceans or lakes where high biological activities occur, the isotopic composition of the dissolved O_2 can be altered by the gas-state air-water exchange, and the interaction of photosynthesis and respiration (Luz and Barkan, 2000; Venkiteswaran et al., 2007; Bao, 2015). The $\delta^{18}\text{O}$ and $\Delta^{17}\text{O}$ values of the dissolved O_2 are different from those of the atmospheric O_2 and the altered isotopic signature is reflected in the sulfate during the formation process such as H_2S oxidation in water bodies, while the signature cannot be quantified because of deficient analytical resolution (Bao, 2015).

5.4. Sulfate from biological processes

The non-labile character of sulfate that preserves the oxygen isotopic composition of source materials after sulfate formation allow us to trace the oxygen sources of sulfate by oxygen isotope analysis (Krouse and Mayer, 2000; Bao, 2015). The oxygen isotope exchange between sulfate and water or minerals occurs at high temperature ($> 350\text{ °C}$) and/or acidic ($> 1\text{ M H}_2\text{SO}_4$ or HCl solution) hydrothermal environments (Kusakabe and Robinson, 1977; Chiba et al., 1981). Under surface conditions, however, the oxygen isotope composition of sulfate can be altered via biological processes such as dissimilatory microbial sulfate reduction by kinetic isotope fractionation (Lloyd, 1967; Aharon

and Fu, 2003) or isotope exchange between sulfate and ambient water (Fritz et al., 1989; Van Stempvoort and Krouse, 1994; Brunner et al., 2005). During microbial sulfate reduction, sulfate is reduced to sulfide and other intermediate sulfur compounds (Canfield, 2004). The $\delta^{18}\text{O}_{\text{sulfate}}$ and $\delta^{34}\text{S}_{\text{sulfate}}$ in natural waters such as aquifers or rivers can increase with the progression of the microbial sulfate reduction process, while the sulfate concentration decreases (Tuttle et al., 2009; Hosono et al., 2011a; Hosono et al., 2014).

The absence of a relationship between the $\delta^{18}\text{O}_{\text{sulfate}}$ and $\delta^{34}\text{S}_{\text{sulfate}}$ might indicate the minor influence of any extensive microbial reduction process on Deception Island water. Previous studies showed the positive relationship between the $\delta^{18}\text{O}_{\text{sulfate}}$ and $\delta^{34}\text{S}_{\text{sulfate}}$ by kinetic isotope exchange during the widespread dissimilatory microbial sulfate reduction process with a slope of 0.25 in natural systems (Mandernack et al., 2003; Tuttle et al., 2009). Brunner et al. (2005), in contrast, suggested that the dissimilatory sulfate reduction process by exchange reaction between the sulfate and ambient water produced none of these linear trends and that a curved line represented the correlation of both isotopes more exactly. Between the $\delta^{18}\text{O}_{\text{sulfate}}$ and $\delta^{34}\text{S}_{\text{sulfate}}$ of Deception Island water, there is no linear and/or curved relationship which might be the signal of widespread microbial reduction process (Fig. 5).

The $\delta^{34}\text{S}_{\text{sulfate}}$ of Deception Island water is positively related to the $\text{Cl}^-/\text{SO}_4^{2-}$ molar ratio, showing the decrease in sulfate concentration with an increase in $\delta^{34}\text{S}_{\text{sulfate}}$ (Fig. 4). Even though the $\delta^{34}\text{S}_{\text{sulfate}}$ and sulfate concentrations show a negative relationship which might be a signal of the microbial reduction process, the maximum $\delta^{34}\text{S}_{\text{sulfate}}$ of Deception Island, 17.3‰, is too low to indicate an influence by the dissimilatory microbial reduction process. The $\delta^{34}\text{S}_{\text{sulfate}}$ of surface waters that are fractionated by dissimilatory microbial sulfate reduction can be high, approaching values between 33.4‰ (Hosono et al., 2011a) to 49.9‰ (Hosono et al., 2014) in the groundwater, and 49.1‰ in the pond at the Antarctica (Sun et al., 2015). The microbial sulfate reduction process, therefore, is considered to have an insignificant impact on the $\delta^{34}\text{S}_{\text{sulfate}}$ of Deception Island water.

5.5. Multiple sulfur isotope composition ($\Delta^{33}\text{S}$ and $\Delta^{36}\text{S}$) of sulfate

Both $\Delta^{33}\text{S}_{\text{sulfate}}$ and $\Delta^{36}\text{S}_{\text{sulfate}}$ of Deception Island water show values close to zero which are completely mass-dependent compositions (Fig. 8). The $\Delta^{17}\text{O}_{\text{sulfate}}$, $\Delta^{33}\text{S}_{\text{sulfate}}$ and $\Delta^{36}\text{S}_{\text{sulfate}}$ data confirmed that the sulfate of Deception Island water was primarily derived from sources fractionated by mass-dependent processes. The homogeneous and mass-dependent $\Delta^{33}\text{S}_{\text{sulfate}}$ (0.00‰ to 0.05‰) and $\Delta^{36}\text{S}_{\text{sulfate}}$

(−0.26‰ to 0.01‰) imply that atmospheric oxidation from SO_2 to sulfate of Deception Island occurred mainly in the troposphere and lower stratosphere where photochemical reaction by UV light (< 220 nm) that might trigger anomalous $\Delta^{33}\text{S}$ and $\Delta^{36}\text{S}$ values is small. This result is consistent with the dominance of mass-dependent fractionated (near zero $\Delta^{33}\text{S}$) background sulfate in the Antarctic ice cores and snow (Alexander et al., 2003; Savarino et al., 2003; Baroni et al., 2008; Kunasek et al., 2010). These studies argued that the near-zero $\Delta^{33}\text{S}_{\text{sulfate}}$ was derived from the background sulfate formed in the troposphere. Savarino et al. (2003), on the other hand, suggested that some eruptive volcanic sulfate could reach higher stratospheric altitudes and be exposed to the stronger UV levels, leading to mass-independent fractionation showing anomalous $\Delta^{33}\text{S}_{\text{sulfate}}$ and $\Delta^{36}\text{S}_{\text{sulfate}}$. Baroni et al. (2008) demonstrated that the $\Delta^{33}\text{S}$ difference of sulfate between ice cores in Antarctica (Dome C and South Pole) preserve a change in sulfur isotope anomaly from positive to negative values during the deposition of mass-independent fractionated sulfate from the stratosphere.

The mass-dependent $\Delta^{33}\text{S}_{\text{sulfate}}$ and $\Delta^{36}\text{S}_{\text{sulfate}}$ of Deception Island water support the suggestion that the volcanic sulfate derives from tropospheric sources rather than stratospheric-scale volcanic activity. The near-zero $\Delta^{33}\text{S}_{\text{sulfate}}$ and $\Delta^{36}\text{S}_{\text{sulfate}}$ enable the exclusion of stratospheric sulfate as one of the main constituents of atmospheric sulfate deposition, of which the $\delta^{34}\text{S}$ is 2.6‰ (Castleman et al., 1974). Due to its low $\delta^{34}\text{S}$, stratospheric sulfate can be one of the candidates for lower end-members in Fig. 4, but near zero $\Delta^{33}\text{S}_{\text{sulfate}}$ and $\Delta^{36}\text{S}_{\text{sulfate}}$ suggest the negligible influence of stratospheric sulfate in Deception Island. This helps to narrow the possible candidates for lower end-member sources to volcanic sulfate from the constantly degassing volcanoes and/or mineral dusts. Kunasek et al. (2010) argued that the contribution of stratospheric sulfate cannot be neglected even if anomalous sulfur isotope compositions are not measured, based on the results of Baroni et al. (2008) that all stratospheric-scale volcanic activities are not identified. In this study, however, both non-anomalous oxygen ($\Delta^{17}\text{O}_{\text{sulfate}}$) and sulfur ($\Delta^{33}\text{S}_{\text{sulfate}}$ and $\Delta^{36}\text{S}_{\text{sulfate}}$) isotopic compositions provide greater support for the opinion that the contribution of stratospheric sulfate to Deception Island is insignificant because stratospheric sulfate formed by the oxidation of SO_2 by stratospheric $\cdot\text{OH}$ can have anomalous $\Delta^{17}\text{O}$ values up to 45‰ (Lyons, 2001; Liang et al., 2006; Zahn et al., 2006).

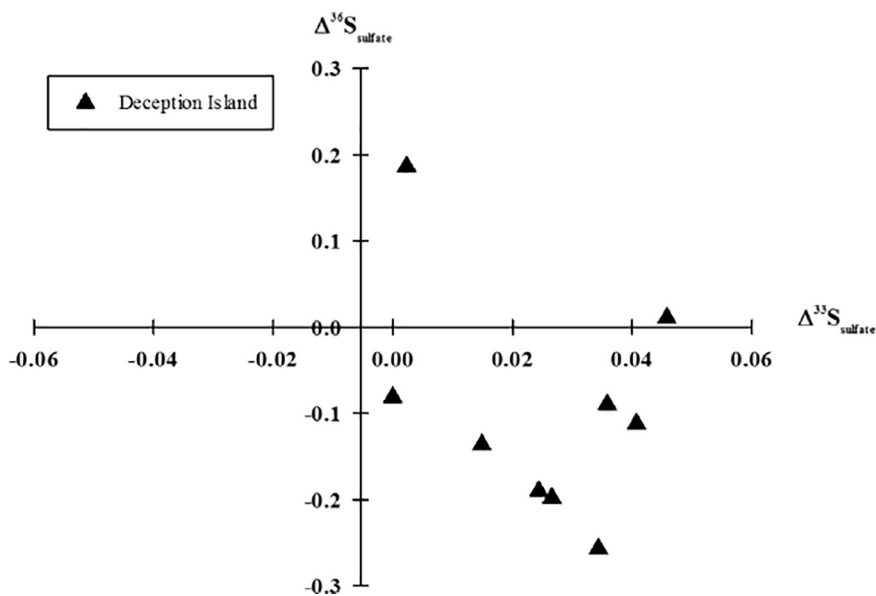


Fig. 8. $\Delta^{33}\text{S}_{\text{sulfate}}$ and $\Delta^{36}\text{S}_{\text{sulfate}}$ from Deception Island water. The homogeneous and mass-dependent $\Delta^{33}\text{S}$ (0.00‰ to 0.05‰) and $\Delta^{36}\text{S}$ (−0.26‰ to 0.01‰) values stress the dominance of the tropospheric oxidation process, which is a result similar to the previous Antarctic ice core and snow studies (Alexander et al., 2003; Baroni et al., 2008; Kunasek et al., 2010). The predominant occurrence of the atmospheric oxidation process in the troposphere confirms the idea that volcanic sulfate was mainly derived from the constantly degassing volcanoes, which had less ability to raise sulfate to the stratosphere where mass-independent fractionation by stronger UV at 220 nm occurs.

6. Conclusions

The multiple oxygen ($\Delta^{17}\text{O}$ and $\delta^{18}\text{O}$) and sulfur ($\delta^{34}\text{S}$, $\Delta^{33}\text{S}$ and $\Delta^{36}\text{S}$) isotope compositions of the dissolved sulfate in the lakes and ponds at Deception Island, Antarctic Peninsulas were measured to trace the sulfate sources and oxidation pathways. The major ion concentration (Na^+ , Ca^{2+} , Cl^- , NO_3^- and SO_4^{2-}) analyses were accompanied with isotope measurements to investigate the surface processes, such as evaporation and mixing, which had an impact on the isotope composition of sulfate. The $\delta^{18}\text{O}_{\text{sulfate}}$ and $\delta^{34}\text{S}_{\text{sulfate}}$ ranged from 8.1‰ to 17.3‰ and from -4.6 ‰ to 0.7‰, respectively. The $\Delta^{17}\text{O}_{\text{sulfate}}$ (-0.22 ‰ to 0.01‰), $\Delta^{33}\text{S}_{\text{sulfate}}$ (0.00‰ to 0.05‰) and $\Delta^{36}\text{S}_{\text{sulfate}}$ (-0.26 ‰ to 0.01‰) represented a non-anomalous composition of the dissolved sulfate. These measurements led to the following conclusions.

- (1) The $\delta^{34}\text{S}_{\text{NSS}}$ value (5.6‰ to 15.9‰) is calculated using an estimated k value (0.07) and sea-salt fractions are from 16% to 43%.
- (2) The plot of $\delta^{34}\text{S}_{\text{sulfate}}$ versus $\text{Cl}^-/\text{SO}_4^{2-}$ molar ratio represented a linear mixing line between two end-members. The possible candidate for the lower end-member is the terrigenous sulfate from volcanoes and mineral dust. The calculated fractions of continental-derived sulfate ($< 10\%$) by the Ca^{2+} concentration suggest their minor influence on the total sulfate budget of Deception Island water.
- (3) The higher end-member sulfate is thought to be the combination of sea-salt aerosol and marine biogenic sources such as DMS. The $\delta^{34}\text{S}_{\text{NSS}}$, which varies little from the $\delta^{34}\text{S}_{\text{sulfate}}$, shows the dominance of marine biogenic sources as the higher end-member.
- (4) The $\delta^{18}\text{O}_{\text{sulfate}}$ of Deception Island water indicates an association with local ambient water. The non-anomalous $\Delta^{17}\text{O}_{\text{sulfate}}$ implies the trivial influence of anomalous atmospheric oxidants such as O_3 and H_2O_2 .
- (5) The two distinct lower values of $\delta^{34}\text{S}_{\text{sulfate}}$ (DCW-2 and DCW-3) could be explained by the input of sulfate via the sulfide oxidation process. The $\delta^{18}\text{O}_{\text{sulfate}}$ and $\delta^{18}\text{O}_{\text{water}}$ of Deception Island water are plotted in the area of the influence of sulfide oxidation process. The slightly negative $\Delta^{17}\text{O}_{\text{sulfate}}$ might be transported from the $\Delta^{17}\text{O}$ signal of molecular oxygen during the sulfide oxidation process.
- (6) The $\Delta^{33}\text{S}_{\text{sulfate}}$ and $\Delta^{36}\text{S}_{\text{sulfate}}$ were completely mass-dependent for Deception Island sulfate, indicating the dominance of mass-dependent atmospheric oxidation processes and support a tropospheric, rather than stratospheric origin for sulfate.

Acknowledgments

This research is supported by the project “PM16030, KOPRI” from the Ministry of Oceans and Fisheries, Korea. The author Y.M. Kim thanks the BK 21 program of the School of Earth and Environmental Sciences, Seoul National University. J.H. Seo acknowledges supports by the Inha University Research Grant (INHA-48580) and by the Korea Energy and Mineral Resources Engineering Program (KEMREP) grant funded by Ministry of Trade, Industry and Energy (MOTIE). The authors wish to thank H. Bao in Louisiana State University for analyzing the oxygen isotope composition ($\delta^{18}\text{O}$ and $\Delta^{17}\text{O}$) of sulfate. We appreciate the staff members at the King Sejong Station at King George Island and Spanish base at Deception Island, Antarctic Peninsula, who supported sampling and research activities in the study area. Constructive comments from three reviewers and the editorial handling of Dr. Johannesson are acknowledged.

References

Aharon, P., Fu, B., 2003. Sulfur and oxygen isotopes of coeval sulfate–sulfide in pore fluids of cold seep sediments with sharp redox gradients. *Chem. Geol.* 195 (1), 201–218.

Alexander, B., Savarino, J., Barkov, N., Delmas, R., Thiemens, M., 2002. Climate driven

changes in the oxidation pathways of atmospheric sulfur. *Geophys. Res. Lett.* 29 (14).

Alexander, B., Thiemens, M., Farquhar, J., Kaufman, A., Savarino, J., Delmas, R., 2003. East Antarctic ice core sulfur isotope measurements over a complete glacial-interglacial cycle. *J. Geophys. Res. Atmos.* 108 (D24).

Alexander, B., Park, R.J., Jacob, D.J., Li, Q., Yantosca, R.M., Savarino, J., Lee, C., Thiemens, M., 2005. Sulfate formation in sea-salt aerosols: constraints from oxygen isotopes. *J. Geophys. Res. Atmos.* 110 (D10).

Alexander, B., Park, R.J., Jacob, D.J., Gong, S., 2009. Transition metal-catalyzed oxidation of atmospheric sulfur: global implications for the sulfur budget. *J. Geophys. Res. Atmos.* 114 (D2).

Alexander, B., Allman, D., Amos, H., Fairlie, T., Dachs, J., Hegg, D.A., Sletten, R.S., 2012. Isotopic constraints on the formation pathways of sulfate aerosol in the marine boundary layer of the subtropical northeast Atlantic Ocean. *J. Geophys. Res. Atmos.* 117 (D6).

Amrani, A., Said-Ahmad, W., Shaked, Y., Kiene, R.P., 2013. Sulfur isotope homogeneity of oceanic DMS and DMS. *Proc. Natl. Acad. Sci.* 110 (46), 18413–18418.

Baker, P., McReath, I., Harvey, M., Roobol, M., Davies, T., 1975. The geology of the South Shetland islands: V. In: *Volcanic Evolution of Deception Island*. 78 British Antarctic Survey.

Balci, N., Shanks, W.C., Mayer, B., Mandernack, K.W., 2007. Oxygen and sulfur isotope systematics of sulfate produced by bacterial and abiotic oxidation of pyrite. *Geochim. Cosmochim. Acta* 71 (15), 3796–3811.

Bao, H., 2006. Purifying barite for oxygen isotope measurement by dissolution and re-precipitation in a chelating solution. *Anal. Chem.* 78 (1), 304–309.

Bao, H., 2015. Sulfate: a time capsule for Earth's O_2 , O_3 , and H_2O . *Chem. Geol.* 395, 108–118.

Bao, H., Reheis, M.C., 2003. Multiple oxygen and sulfur isotopic analyses on water-soluble sulfate in bulk atmospheric deposition from the southwestern United States. *J. Geophys. Res. Atmos.* 108 (D14).

Bao, H., Thiemens, M.H., 2000. Generation of O_2 from BaSO_4 using a CO_2 -laser fluorination system for simultaneous analysis of $\delta^{18}\text{O}$ and $\delta^{17}\text{O}$. *Anal. Chem.* 72 (17), 4029–4032.

Baraldo, A., Rinaldi, C., 2000. Stratigraphy and structure of Deception Island, south Shetland Islands, Antarctica. *J. S. Am. Earth Sci.* 13 (8), 785–796.

Barkan, E., Luz, B., 2005. High precision measurements of $^{17}\text{O}/^{16}\text{O}$ and $^{18}\text{O}/^{16}\text{O}$ ratios in H_2O . *Rapid Commun. Mass Spectrom.* 19 (24), 3737–3742.

Baroni, M., Savarino, J., Cole-Dai, J., Rai, V.K., Thiemens, M.H., 2008. Anomalous sulfur isotope compositions of volcanic sulfate over the last millennium in Antarctic ice cores. *J. Geophys. Res. Atmos.* 113 (D20).

Berner, E.K., Berner, R.A., 2012. *Global Environment: Water, air, and Geochemical Cycles*. Princeton University Press.

Bottrell, S., Tellam, J., Bartlett, R., Hughes, A., 2008. Isotopic composition of sulfate as a tracer of natural and anthropogenic influences on groundwater geochemistry in an urban sandstone aquifer, Birmingham, UK. *Appl. Geochem.* 23 (8), 2382–2394.

Brenot, A., Nègre, P., Petelet-Giraud, E., Millot, R., Malcuit, E., 2015. Insights from the salinity origins and interconnections of aquifers in a regional scale sedimentary aquifer system (Adour-Garonne district, SW France): contributions of $\delta^{34}\text{S}$ and $\delta^{18}\text{O}$ from dissolved sulfates and the $^{87}\text{Sr}/^{86}\text{Sr}$ ratio. *Appl. Geochem.* 53, 27–41.

Brunner, B., Bernasconi, S.M., Kleikemper, J., Schroth, M.H., 2005. A model for oxygen and sulfur isotope fractionation in sulfate during bacterial sulfate reduction processes. *Geochim. Cosmochim. Acta* 69 (20), 4773–4785.

Calhoun, J.A., Bates, T.S., Charlson, R.J., 1991. Sulfur isotope measurements of sub-micrometer sulfate aerosol particles over the Pacific Ocean. *Geophys. Res. Lett.* 18 (10), 1877–1880.

Canfield, D.E., 2004. The evolution of the earth surface sulfur reservoir. *Am. J. Sci.* 304 (10), 839–861.

Castleman, A., Munkelwitz, H., Manowitz, B., 1974. Isotopic studies of the sulfur component of the stratospheric aerosol layer 1. 2. *Tellus* 26 (1–2), 222–234.

Chen, S., Guo, Z., Guo, Z., Guo, Q., Zhang, Y., Zhu, B., Zhang, H., 2017. Sulfur isotopic fractionation and its implication: sulfate formation in PM 2.5 and coal combustion under different conditions. *Atmos. Res.* 194, 142–149.

Chiba, H., Kusakabe, M., Hirano, S.-I., Matsuo, S., Somiya, S., 1981. Oxygen isotope fractionation factors between anhydrite and water from 100 to 550 °C. *Earth Planet. Sci. Lett.* 53 (1), 55–62.

Delmas, R.J., Legrand, M., Aristarain, A.J., Zanolini, F., 1985. Volcanic deposits in Antarctic snow and ice. *J. Geophys. Res. Atmos.* 90 (D7), 12901–12920.

Dominguez, G., Jackson, T., Brothers, L., Barnett, B., Nguyen, B., Thiemens, M.H., 2008. Discovery and measurement of an isotopically distinct source of sulfate in Earth's atmosphere. *Proc. Natl. Acad. Sci.* 105 (35), 12769–12773.

Farquhar, J., Bao, H., Thiemens, M., 2000. Atmospheric influence of Earth's earliest sulfur cycle. *Science* 289 (5480), 756–758.

Fogelman, K.D., Walker, D.M., Margerum, D.W., 1989. Nonmetal redox kinetics: hypochlorite and hypochlorous acid reactions with sulfite. *Inorg. Chem.* 28 (6), 986–993.

Fritz, P., Basharmal, G., Drimmie, R., Ibsen, J., Qureshi, R., 1989. Oxygen isotope exchange between sulphate and water during bacterial reduction of sulphate. *Chem. Geol. Isot. Geosci. Sec.* 79 (2), 99–105.

Guo, Z., Li, Z., Farquhar, J., Kaufman, A.J., Wu, N., Li, C., Dickerson, R.R., Wang, P., 2010. Identification of sources and formation processes of atmospheric sulfate by sulfur isotope and scanning electron microscope measurements. *J. Geophys. Res. Atmos.* 115 (D7).

Harris, E., Sinha, B., Hoppe, P., Crowley, J., Ono, S., Foley, S., 2012. Sulfur isotope fractionation during oxidation of sulfur dioxide: gas-phase oxidation by OH radicals and aqueous oxidation by H_2O_2 , O_3 and iron catalysis. *Atmos. Chem. Phys.* 12 (1), 407–423.

Harris, E., Sinha, B., van Pinxteren, D., Tilgner, A., Fomba, K.W., Schneider, J., Roth, A., Gnauk, T., Fahlbusch, B., Mertes, S., 2013. Enhanced role of transition metal ion

- catalysis during in-cloud oxidation of SO₂. *Science* 340 (6133), 727–730.
- Heidel, C., Tichomirowa, M., Junghans, M., 2013. Oxygen and sulfur isotope investigations of the oxidation of sulfide mixtures containing pyrite, galena, and sphalerite. *Chem. Geol.* 342, 29–43.
- Holland, H.D., 1978. *The Chemistry of the Atmosphere and Oceans* (v. 1).
- Hong, Y.-L., Kim, G., 2005. Measurement of cosmogenic ³⁵S activity in rainwater and lake water. *Anal. Chem.* 77 (10), 3390–3393.
- Hosono, T., Delinom, R., Nakano, T., Kagabu, M., Shimada, J., 2011a. Evolution model of δ³⁴S and δ¹⁸O in dissolved sulfate in volcanic fan aquifers from recharge to coastal zone and through the Jakarta urban area, Indonesia. *Sci. Total Environ.* 409 (13), 2541–2554.
- Hosono, T., Wang, C.-H., Umezawa, Y., Nakano, T., Onodera, S.-I., Nagata, T., Yoshimizu, C., Tayasu, I., Taniguchi, M., 2011b. Multiple isotope (H, O, N, S and Sr) approach elucidates complex pollution causes in the shallow groundwaters of the Taipei urban area. *J. Hydrol.* 397 (1), 23–36.
- Hosono, T., Lorphensriand, O., Onodera, S.-I., Okawa, H., Nakano, T., Yamanaka, T., Tsujimura, M., Taniguchi, M., 2014. Different isotopic evolutionary trends of δ³⁴S and δ¹⁸O compositions of dissolved sulfate in an anaerobic deltaic aquifer system. *Appl. Geochem.* 46, 30–42.
- Jenkins, K.A., Bao, H., 2006. Multiple oxygen and sulfur isotope compositions of atmospheric sulfur in Baton Rouge, LA, USA. *Atmos. Environ.* 40 (24), 4528–4537.
- Johnston, J.C., Thiemens, M.H., 1997. The isotopic composition of tropospheric ozone in three environments. *J. Geophys. Res.* Atmos. 102 (D21), 25395–25404.
- Jonsell, U., Hansson, M.E., MÖRTH, C., Torssander, P., 2005. Sulfur isotopic signals in two shallow ice cores from Dronning Maud land, Antarctica. *Tellus B* 57 (4), 341–350.
- Jovic, S.M., Guido, D.M., Schalamuk, I.B., Ríos, F.J., Tassinari, C.C., Recio, C., 2011. Pingüino in-bearing polymetallic vein deposit, Deseado Massif, Patagonia, Argentina: characteristics of mineralization and ore-forming fluids. *Mineral. Deposita* 46 (3), 257–271.
- Killingsworth, B.A., Bao, H., 2015. Significant human impact on the flux and δ³⁴S of sulfate from the Largest River in North America. *Environ. Sci. Technol.* 49 (8), 4851–4860.
- Krouse, H.R., Mayer, B., 2000. Sulphur and Oxygen Isotopes in Sulphate, Environmental Tracers in Subsurface Hydrology. Springerpp. 195–231.
- Kunasek, S., Alexander, B., Steig, E., Sofen, E., Jackson, T., Thiemens, M., McConnell, J., Gleason, D., Amos, H., 2010. Sulfate sources and oxidation chemistry over the past 230 years from sulfur and oxygen isotopes of sulfate in a West Antarctic ice core. *J. Geophys. Res.* Atmos. 115 (D18).
- Kusakabe, M., Robinson, B.W., 1977. Oxygen and sulfur isotope equilibria in the BaSO₄–H₂O system from 110 to 350 °C and applications. *Geochim. Cosmochim. Acta* 41 (8), 1033–1040.
- Kusakabe, M., Nagao, K., Ohba, T., Seo, J.H., Park, S.-H., Lee, J.I., Park, B.-K., 2009. Noble gas and stable isotope geochemistry of thermal fluids from Deception Island, Antarctica. *Antarct. Sci.* 21 (03), 255.
- Lanfranchini, M.E., Etcheverry, R.O., de Barrio, R.E., Hernández, C.R., 2013. Precious metal-bearing epithermal deposits in western Patagonia (NE Lago Fontana region), Argentina. *J. S. Am. Earth Sci.* 43, 86–100.
- Lee, M.J., Lee, J.I., Choe, W.H., Park, C.-H., 2008. Trace element and isotopic evidence for temporal changes of the mantle sources in the South Shetland Islands, Antarctica. *Geochim. J.* 42 (2), 207–219.
- Legrand, M., Hammer, C., De Angelis, M., Savarino, J., Delmas, R., Clausen, H., Johnsen, S.J., 1997. Sulfur-containing species (methanesulfonate and SO₄) over the last climatic cycle in the Greenland Ice Core Project (central Greenland) ice core. *J. Geophys. Res.* Oceans 102 (C12), 26663–26679.
- Li, X., Gan, Y., Zhou, A., Liu, Y., 2015. Relationship between water discharge and sulfate sources of the Yangtze River inferred from seasonal variations of sulfur and oxygen isotopic compositions. *J. Geochem. Explor.* 153, 30–39.
- Liang, M.C., Irion, F.W., Weibel, J.D., Miller, C.E., Blake, G.A., Yung, Y.L., 2006. Isotopic composition of stratospheric ozone. *J. Geophys. Res.* Atmos. 111 (D2).
- Lim, C., Jang, J., Lee, I., Kim, G., Lee, S.-M., Kim, Y., Kim, H., Kaufman, A.J., 2014. Sulfur isotope and chemical compositions of the wet precipitation in two major urban areas, Seoul and Busan, Korea. *J. Asian Earth Sci.* 79, 415–425.
- Lloyd, R., 1968. Oxygen isotope behavior in the sulfate-water system. *J. Geophys. Res.* 73 (18), 6099–6110.
- Lloyd, R.M., 1967. Oxygen-18 composition of oceanic sulfate. *Science* 156 (3779), 1228–1231.
- Luz, B., Barkan, E., 2000. Assessment of oceanic productivity with the triple-isotope composition of dissolved oxygen. *Science* 288 (5473), 2028–2031.
- Lyons, J.R., 2001. Transfer of mass-independent fractionation in ozone to other oxygen-containing radicals in the atmosphere. *Geophys. Res. Lett.* 28 (17), 3231–3234.
- Machado, A., Chemale, F., Conceição, R.V., Kawakita, K., Morata, D., Oteiza, O., Van Schmus, W.R., 2005. Modeling of subduction components in the genesis of the Mesozoic igneous rocks from the South Shetland Arc, Antarctica. *Lithos* 82 (3), 435–453.
- Manderack, K.W., Krouse, H.R., Skei, J.M., 2003. A stable sulfur and oxygen isotopic investigation of sulfur cycling in an anoxic marine basin, Framvaren Fjord, Norway. *Chem. Geol.* 195 (1), 181–200.
- McCabe, J.R., Savarino, J., Alexander, B., Gong, S., Thiemens, M.H., 2006. Isotopic constraints on non-photochemical sulfate production in the Arctic winter. *Geophys. Res. Lett.* 33 (5).
- Minikin, A., Wagenbach, D., Graf, V., Kipfstuhl, J., 1994. Spatial and seasonal variations of the snow chemistry at the central Filchner-Ronne ice shelf, Antarctica. *Ann. Glaciol.* 20 (1), 283–290.
- Moreira, P., Fernández, R.R., 2015. La Josefina Au–Ag deposit (Patagonia, Argentina): a Jurassic epithermal deposit formed in a hot spring environment. *Ore Geol. Rev.* 67, 297–313.
- Morin, S., Savarino, J., Bekki, S., Gong, S., Bottenheim, J., 2007. Signature of Arctic surface ozone depletion events in the isotope anomaly (Δ¹⁷O) of atmospheric nitrate. *Atmos. Chem. Phys.* 7 (5), 1451–1469.
- Nakai, N., Jensen, M., 1964. The kinetic isotope effect in the bacterial reduction and oxidation of sulfur. *Geochim. Cosmochim. Acta* 28 (12), 1893–1912.
- Nghiem, S., Martin, S., Perovich, D., Kwok, R., Drucker, R., Gow, A., 1997. A laboratory study of the effect of frost flowers on C band radar backscatter from sea ice. *J. Geophys. Res.* Oceans 102 (C2), 3357–3370.
- Nielsen, H., 1974. Isotopic composition of the major contributors to atmospheric sulfur. *Tellus* 26 (1–2), 213–221.
- Norman, A.L., Belzer, W., Barrie, L., 2004. Insights into the biogenic contribution to total sulphate in aerosol and precipitation in the Fraser Valley afforded by isotopes of sulphur and oxygen. *J. Geophys. Res.* Atmos. 109 (D5).
- Oduro, H., Van Alstyne, K.L., Farquhar, J., 2012. Sulfur isotope variability of oceanic DMS₂ generation and its contributions to marine biogenic sulfur emissions. *Proc. Natl. Acad. Sci.* 109 (23), 9012–9016.
- Otero, N., Soler, A., Canals, A., 2008. Controls of δ³⁴S and δ¹⁸O in dissolved sulphate: learning from a detailed survey in the Llobregat River (Spain). *Appl. Geochem.* 23 (5), 1166–1185.
- Patris, N., Delmas, R.J., Jouzel, J., 2000. Isotopic signatures of sulfur in shallow Antarctic ice cores. *J. Geophys. Res.* Atmos. 105 (D6), 7071–7078.
- Patris, N., Delmas, R., Legrand, M., De Angelis, M., Ferron, F.A., Stiévenard, M., Jouzel, J., 2002. First sulfur isotope measurements in central Greenland ice cores along the preindustrial and industrial periods. *J. Geophys. Res.* Atmos. 107 (D11).
- Perovich, D.K., Richter-Menge, J.A., 1994. Surface characteristics of lead ice. *J. Geophys. Res.* Oceans 99 (C8), 16341–16350.
- Pruett, L.E., Kreutz, K.J., Wadleigh, M., Mayewski, P.A., Kurbatov, A., 2004. Sulfur isotopic measurements from a West Antarctic ice core: implications for sulfate source and transport. *Ann. Glaciol.* 39 (1), 161–168.
- Raidla, V., Kirsimäe, K., Ivask, J., Kaup, E., Knöller, K., Marandi, A., Martma, T., Vaikmäe, R., 2014. Sulphur isotope composition of dissolved sulphate in the Cambrian–Vendian aquifer system in the northern part of the Baltic Artesian Basin. *Chem. Geol.* 383, 147–154.
- Rankin, A., Auld, V., Wolff, E., 2000. Frost flowers as a source of fractionated sea salt aerosol in the polar regions. *Geophys. Res. Lett.* 27 (21), 3469–3472.
- Rees, C., Jenkins, W., Monster, J., 1978. The sulphur isotopic composition of ocean water sulphate. *Geochim. Cosmochim. Acta* 42 (4), 377–381.
- Richardson, C., 1976. Phase relationships in sea ice as a function of temperature. *J. Glaciol.* 17 (77), 507–519.
- Rock, L., Mayer, B., 2009. Identifying the influence of geology, land use, and anthropogenic activities on riverine sulfate on a watershed scale by combining hydrometric, chemical and isotopic approaches. *Chem. Geol.* 262 (3), 121–130.
- Romero, A.B., Thiemens, M.H., 2003. Mass-independent sulfur isotopic compositions in present-day sulfate aerosols. *J. Geophys. Res.* Atmos. 108 (D16).
- Savarino, J.S., Thiemens, M.H., 1999. Mass-independent oxygen isotope (16O, 17O, 18O) fractionation found in H₂O x O₂ reactions. *J. Phys. Chem. A* 103 (46), 9221–9229.
- Savarino, J., Lee, C.C., Thiemens, M.H., 2000. Laboratory oxygen isotopic study of sulfur (IV) oxidation: origin of the mass-independent oxygen isotopic anomaly in atmospheric sulfates and sulfate mineral deposits on Earth. *J. Geophys. Res.* Atmos. 105 (D23), 29079–29088.
- Savarino, J., Romero, A., Cole-Dai, J., Bekki, S., Thiemens, M., 2003. UV induced mass-independent sulfur isotope fractionation in stratospheric volcanic sulfate. *Geophys. Res. Lett.* 30 (21).
- Schwartz, S.E., 1987. Aqueous-phase reactions in clouds, the chemistry of acid rain. ACS symposium series. Am. Chem. Soc. 93–108.
- Smellie, J., 2001. Lithostratigraphy and volcanic evolution of Deception Island, south Shetland Islands. *Antarct. Sci.* 13 (02), 188–209.
- Smellie, J., López-Martínez, J., 2000. Geological map of Deception Island. In: Series BAS GEOMAP, Sheet.
- Smellie, J.L., Pankhurst, R., Thomson, M., Davies, R., 1984. The Geology of the South Shetland Islands: VI. In: Stratigraphy, Geochemistry and Evolution, 87. British Antarctic Survey.
- Sofen, E., Alexander, B., Kunasek, S., 2011. The impact of anthropogenic emissions on atmospheric sulfate production pathways, oxidants, and ice core Δ¹⁷O (SO₄ 2–). *Atmos. Chem. Phys.* 11 (7), 3565–3578.
- Stockwell, W.R., Calvert, J.G., 1983. The mechanism of the HO-SO₂ reaction. *Atmos. Environ.* 17 (11), 2231–2235 (1967).
- Sun, T., Socki, R.A., Bish, D.L., Harvey, R.P., Bao, H., Niles, P.B., Caviccholi, R., Tonui, E., 2015. Lost cold Antarctic deserts inferred from unusual sulfate formation and isotope signatures. *Nat. Commun.* 6.
- Taylor, B.E., Wheeler, M.C., Nordstrom, D.K., 1984. Stable isotope geochemistry of acid mine drainage: experimental oxidation of pyrite. *Geochim. Cosmochim. Acta* 48 (12), 2669–2678.
- Thode, H., Monster, J., Dunford, H., 1961. Sulphur isotope geochemistry. *Geochim. Cosmochim. Acta* 25 (3), 159–174.
- Thompson, A.M., 1992. The oxidizing capacity of the Earth's atmosphere: probable past and future changes. *Science* 256 (5060), 1157–1165.
- Troy, R.C., Margerum, D.W., 1991. Non-metal redox kinetics: Hypobromite and hypobromous acid reactions with iodide and with sulfite and the hydrolysis of bromosulfate. *Inorg. Chem.* 30 (18), 3538–3543.
- Tuttle, M.L.W., Breit, G.N., Cozzarelli, I.M., 2009. Processes affecting δ³⁴S and δ¹⁸O values of dissolved sulfate in alluvium along the Canadian River, central Oklahoma, USA. *Chem. Geol.* 265 (3–4), 455–467.
- Van Stempvoort, D., Krouse, H., 1994. Controls of ¹⁸O in sulfate: review of experimental data and application to specific environments, ACS symposium series. Am.

- Chem. Soc. 446.
- Venkiteswaran, J.J., Wassenaar, L.I., Schiff, S.L., 2007. Dynamics of dissolved oxygen isotopic ratios: a transient model to quantify primary production, community respiration, and air–water exchange in aquatic ecosystems. *Oecologia* 153 (2), 385–398.
- Vicars, W.C., Savarino, J., 2014. Quantitative constraints on the $\Delta 17\text{O}$ signature of surface ozone: ambient measurements from 50°N to 50°S using the nitrite-coated filter technique. *Geochim. Cosmochim. Acta* 135, 270–287.
- Vogt, R., Crutzen, P.J., Sander, R., 1996. A mechanism for halogen release from sea-salt aerosol in the remote marine boundary layer. *Nature* 383 (6598), 327–330.
- von Glasow, R., Sander, R., Bott, A., Crutzen, P.J., 2002. Modeling halogen chemistry in the marine boundary layer 2. Interactions with sulfur and the cloud-covered MBL. *J. Geophys. Res. Atmos.* 107, D17.
- Wagenbach, D., Ducroz, F., Mulvaney, R., Keck, L., Minikin, A., Legrand, M., Hall, J., Wolff, E., 1998. Sea-salt aerosol in coastal Antarctic regions. *J. Geophys. Res. Atmos.* 103 (D9), 10961–10974.
- Weaver, S.D., Saunders, A.D., Pankhurst, R.J., Tarney, J., 1979. A geochemical study of magmatism associated with the initial stages of back-arc spreading. *Contrib. Mineral. Petrol.* 68 (2), 151–169.
- Yuan, F., Mayer, B., 2012. Chemical and isotopic evaluation of sulfur sources and cycling in the Pecos River, New Mexico, USA. *Chem. Geol.* 291, 13–22.
- Zahn, A., Franz, P., Bechtel, C., Groß, J.-U., Röckmann, T., 2006. Modelling the budget of middle atmospheric water vapour isotopes. *Atmos. Chem. Phys.* 6 (8), 2073–2090.